Supporting Information:

Expanding the Toolbox for Supramolecular Chemistry: Probing Host-Guest Interactions with *in situ* FTIR Spectroscopy

Shiva Moaven,[1] Douglas A. Vander Griend,[2] Darren W. Johnson,[1,] Michael D. Pluth[1,*]*

[1] Department of Chemistry and Biochemistry, Materials Science Institute, 1253 University of Oregon, Eugene, OR 97403, United States

[2] Department of Chemistry and Biochemistry, Calvin University, Grand Rapids, MI 49546, USA

Corresponding authors: pluth@uoregon.edu, dwj@uoregon.edu

Table of Contents

Experimental Details

S1.1 General Methods

General reagents and reaction starting materials were used as purchased. Anhydrous acetone (500 mL, ACS grade) was obtained by heating at 50 °C and stirring over K_2CO_3 (15 g, ACS grade) for 16 hours, distilling under N_2, and storing over activated 3 Å molecular sieves inside an N_2 glovebox. Anhydrous acetonitrile (MeCN) was obtained by passing the HPLC grade over a bed of activated molecular sieves in a commercial (Pure Process Technology) solvent purification system (SPS). Deuterated solvents were purchased from Cambridge Isotopes Laboratory and degassed using three freeze-pump-thaw cycles before being transferred onto freshly activated 3 Å molecular sieves inside the glovebox. 1,3-*bis*(2,6-Diisopropylphenyl)imidazoliumchloride (H-IPr·Cl), 1,3-*bis*(2,6-diisopropylphenyl)imidazoliumhexafluorophosphate (H-IPr·PF_6), and 1,1′,1″-(nitrilotri(ethane-2,1-diyl))tri(3-(4-trifluoromethyl)phenyl)urea) (*p*-CF_3-tren-trisurea) were prepared according as described previously.[1–3] Air or moisture-sensitive manipulations were performed in a nitrogen-purged inert atmosphere box. All NMR spectra were collected at 25 °C on a Varian Inova 500 MHz NMR spectrometer. All solid-state IR spectra were obtained using a Nicolet 6700 FT-IR spectrometer equipped with an ATR accessory.

S1.2 Synthesis

S1.2.1 Preparation of D-IPr·PF_6

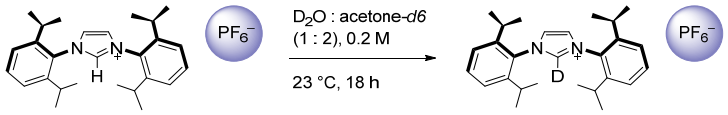

Scheme S1. Reaction scheme for deuterium exchange on H-IPr·PF_6.

The following procedure was adapted from a previous report.[4] In a 25 mL round bottom flask, H-IPr·PF_6 (1.100 g, 2.058 mmol) was dissolved in a 10 mL mixture of 1:2 D_2O:acetone-d_6 and stirred at 23 °C for 12 hours. The reaction mixture was then concentrated to ~4 mL and stored at −20 °C. After 18 hours, the compound had crystallized, and the resultant crystals were collected by filtration and dried in a vacuum oven at 60 °C for 12 hours. The final product was stored inside a N_2-filled glovebox. Yield 870 mg (79%). ^{1}H NMR (500 MHz, acetone-d_6, δ): 1.29 (dd, J = 26.8, 6.9 Hz, 24H), 2.60 (p, J = 6.8 Hz, 4H), 7.56 (d, J = 7.56 Hz, 4H), 7.71 (t, J = 7.9 Hz, 2H), 8.45 (s, *2*H), 9.82 (t, J = 1.6 Hz, 0.05H). ^{2}H NMR (76.8 MHz, acetone-d_6, δ): 9.80 (s, broad). FTIR (ATR, cm^{-1}) 3179, 3158 ($\nu_{C–H}$, w); 2966, 2930, 2870 ($\nu_{C–H}$, m to w); 2358 ($\nu_{C–D}$, w); 1518 ($\nu_{C=N}$, m); 1610 ($\nu_{C=C}$, s), 1454 ($\delta_{C–H}$, m).

S1.3 Spectroscopic Data

S1.3.1 ^{1}H NMR

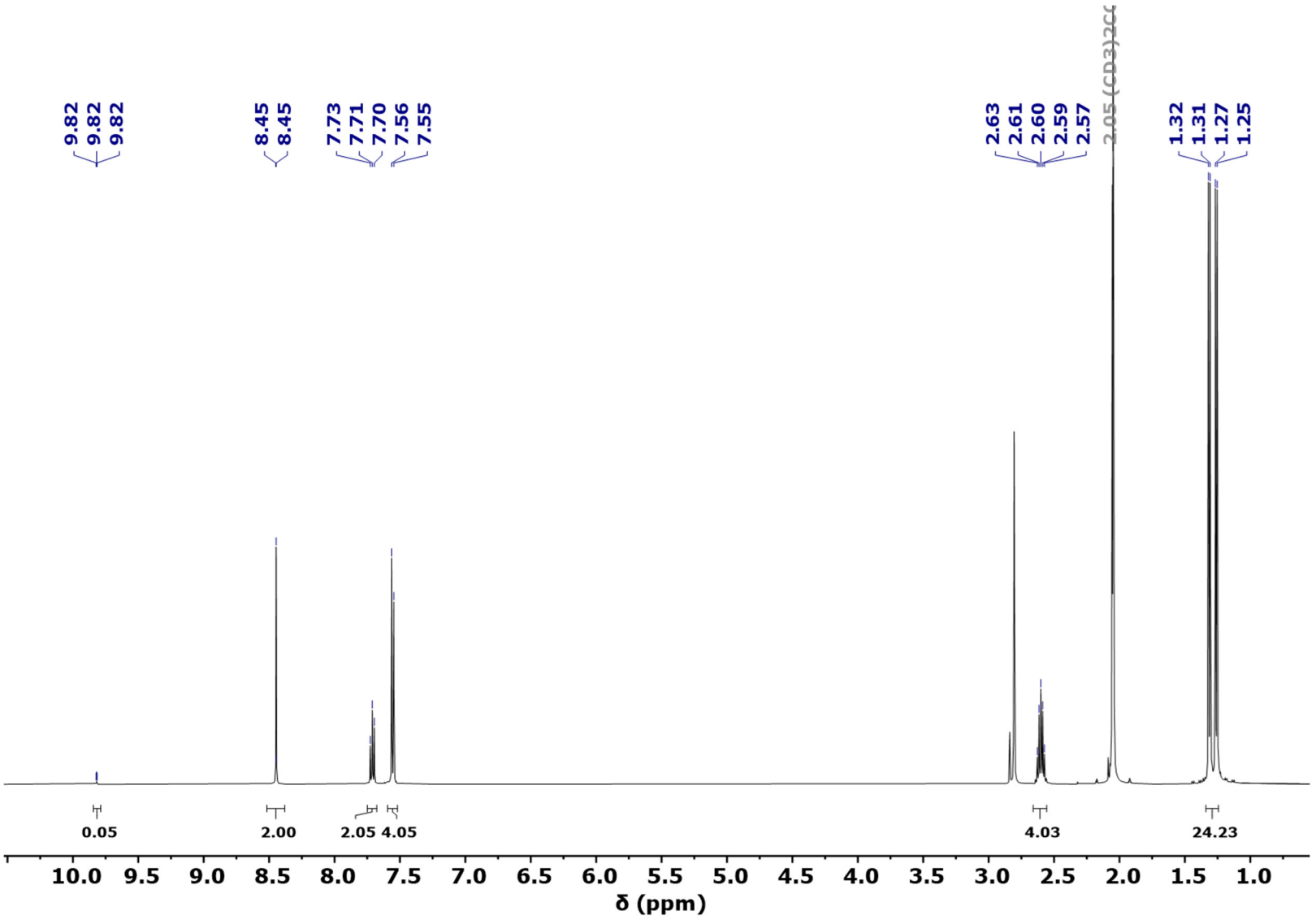

Figure S1. ^{1}H NMR spectrum (500 MHz, acetone-d_6) of D-IPr·PF_6 at 298 K.

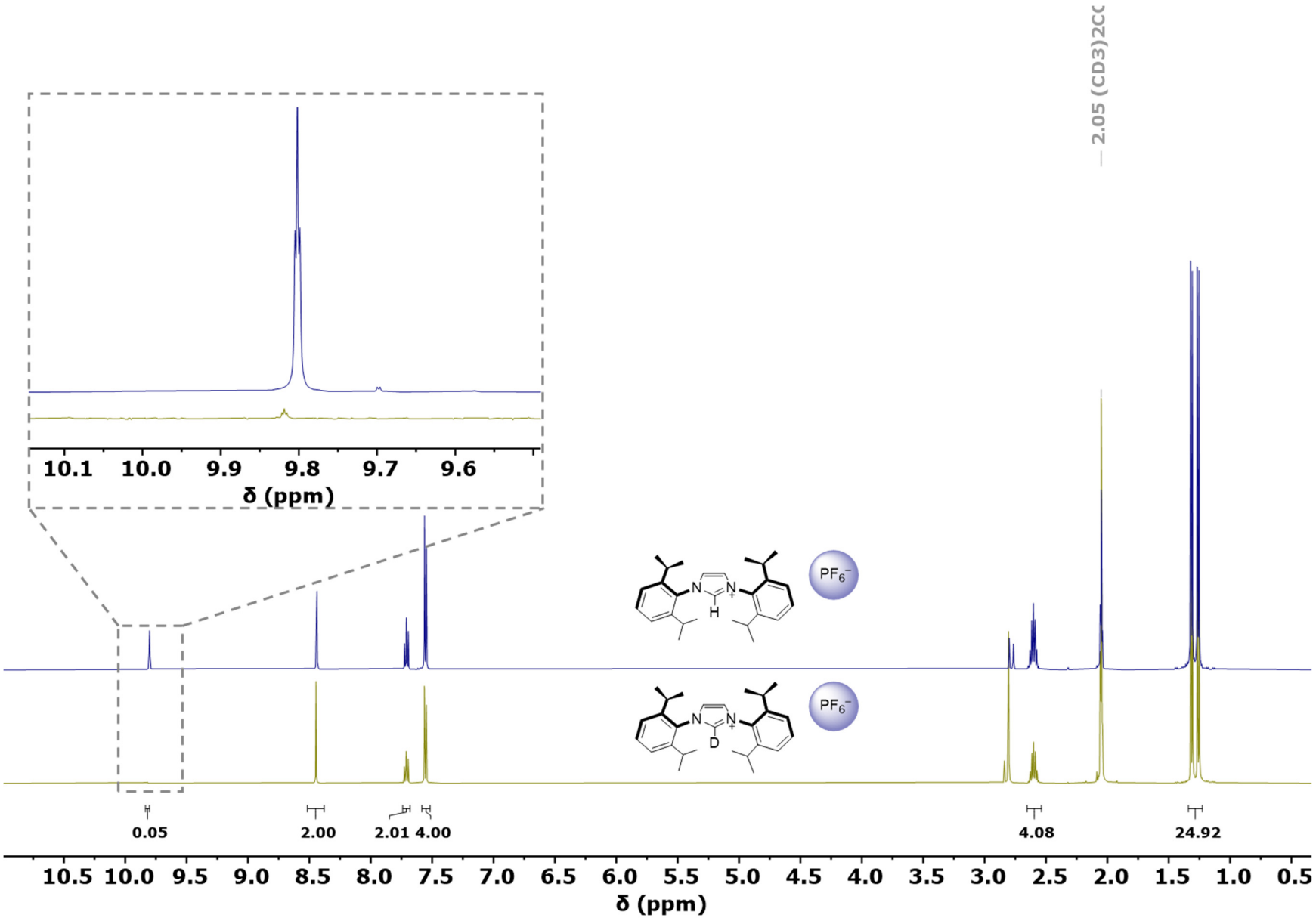

Figure S2. Comparison of the ^{1}H NMR spectra of H-IPr·PF_6 (top trace) and D-IPr·PF_6 (bottom trace) in acetone-d_6 at 298 K. Expansion is the residual signal of the proton on the C-2 position.

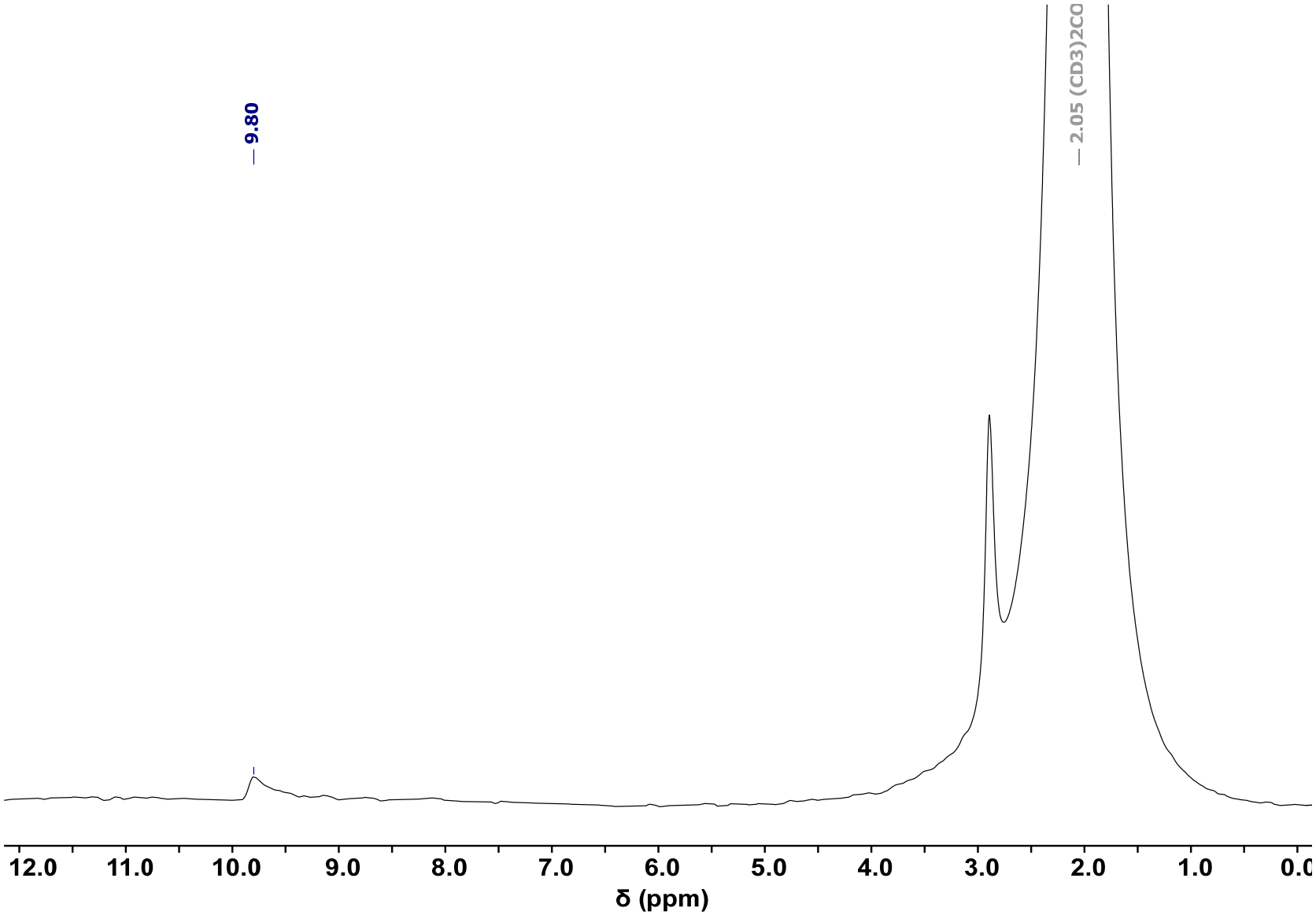

Figure S3. ^{2}H NMR spectrum (76.8 MHz, acetone-d_6) of D-IPr·PF_6 at 298 K.

S1.3.2 *in situ* FTIR titrations

The *in situ* FTIR titration data were collected at 25 °C or 23 °C on a Mettler Toledo model 702 ReactIR instrument. All *in situ* FTIR measurements were performed with the ReactIR probe inside an N_2-purged Schlenk tube equipped with a septum, gas inlet, and adapter for the ReactIR probe (see Figure S4). The temperature was maintained using a temperature-controlled aluminum block padded with glass wool. All solution transfers and guest additions were performed with gas-tight syringes. All samples were prepared inside a nitrogen-filled glovebox. Before each titration experiment, a background spectrum of the degassed solvent or solution mixture was collected. Stock solutions of the D/H-IPr·PF_6 and *p*-CF_3-tren-trisurea receptors were prepared in anhydrous acetone and 20% DMSO in MeCN, respectively. Experiments with the halogen bond donor (NBS) were performed under ambient conditions using ACS grade MeCN and protected from light with aluminum foil. For each *in situ* FTIR trial 3.0 mL of the host solution was transferred into the septa sealed Schlenk flask. To maintain a constant host concentration during the titration process, each guest titrant (TBACl, TBABr, TBAI, $TBAHSO_4$, $TBANO_3$, TBAOCN) was added to 1 mL of the host solution at the desired concentration.[5] After each guest addition, the resultant host-guest solution was allowed to stir for at least one minute for equilibration and then FTIR spectrum would be collected.

Safety Caution! *N*-Bromosuccinimide (NBS) is a corrosive and oxidizing compound and should be handled with care. All solutions containing NBS were quenched with an excess of sodium thiosulfate in water prior to disposal.

Binding affinities from the FTIR data were measured using parametric equilibrium-restricted global analysis (PERGA) using the SIVVU program.[6] Different models were tested to confirm the best fit to the data. Data fitting was performed without modeling activity estimations. Titrations

were performed in triplicate, where the final values reported in each table are the average of K_a and the histogram of combined 95% confidence intervals for the three titrations.[7] Activities could potentially be modeled as something other than unity according to various constructs (Scatchard, Debye-Hückel, etc.), but doing so only results in a small, concerted shift in the log K values that does not improve the fit to the data. The logarithm of activity coefficients are rendered as additive constants in the expression of log K values. Therefore, the newer versions of SIVVU do not include activity coefficients, because including such activity coefficients would just shift the K_a values, but not lead to convergence across different methods.

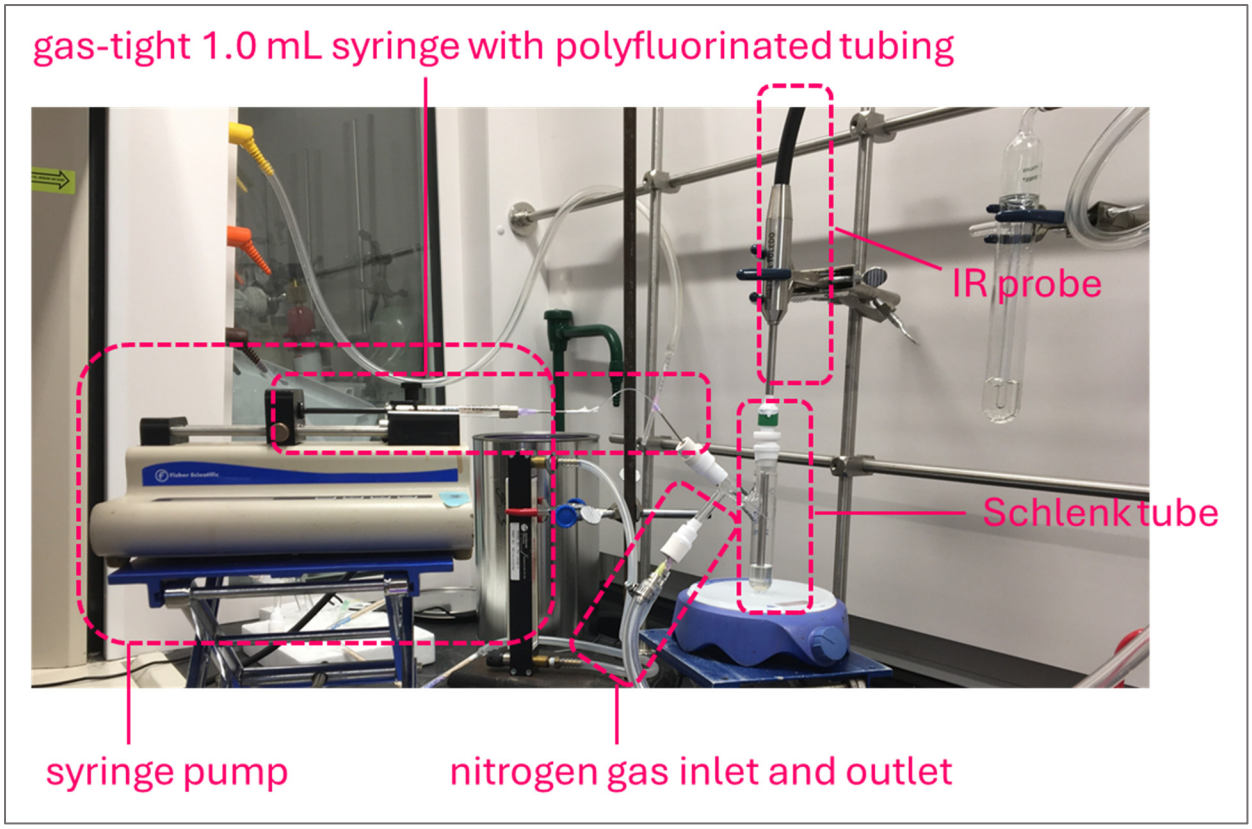

Figure S4. The general setup for the *in situ* FTIR experiments.S1.3.2.1 Details and results of *in situ* FTIR titration for D-IPr·PF_6 and TBACl

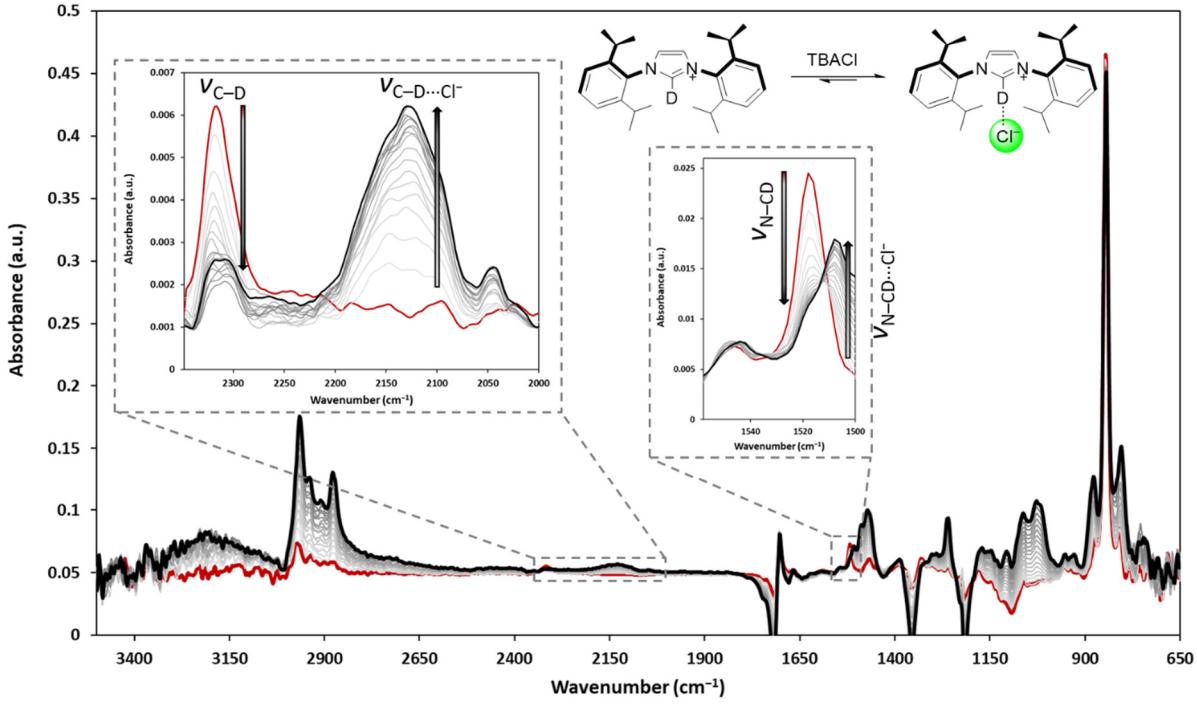

Figure S5. Full *in situ* FTIR titration spectra of D-IPr·PF_6 (48.3 mM) and TBACl in dry acetone at 296 K.

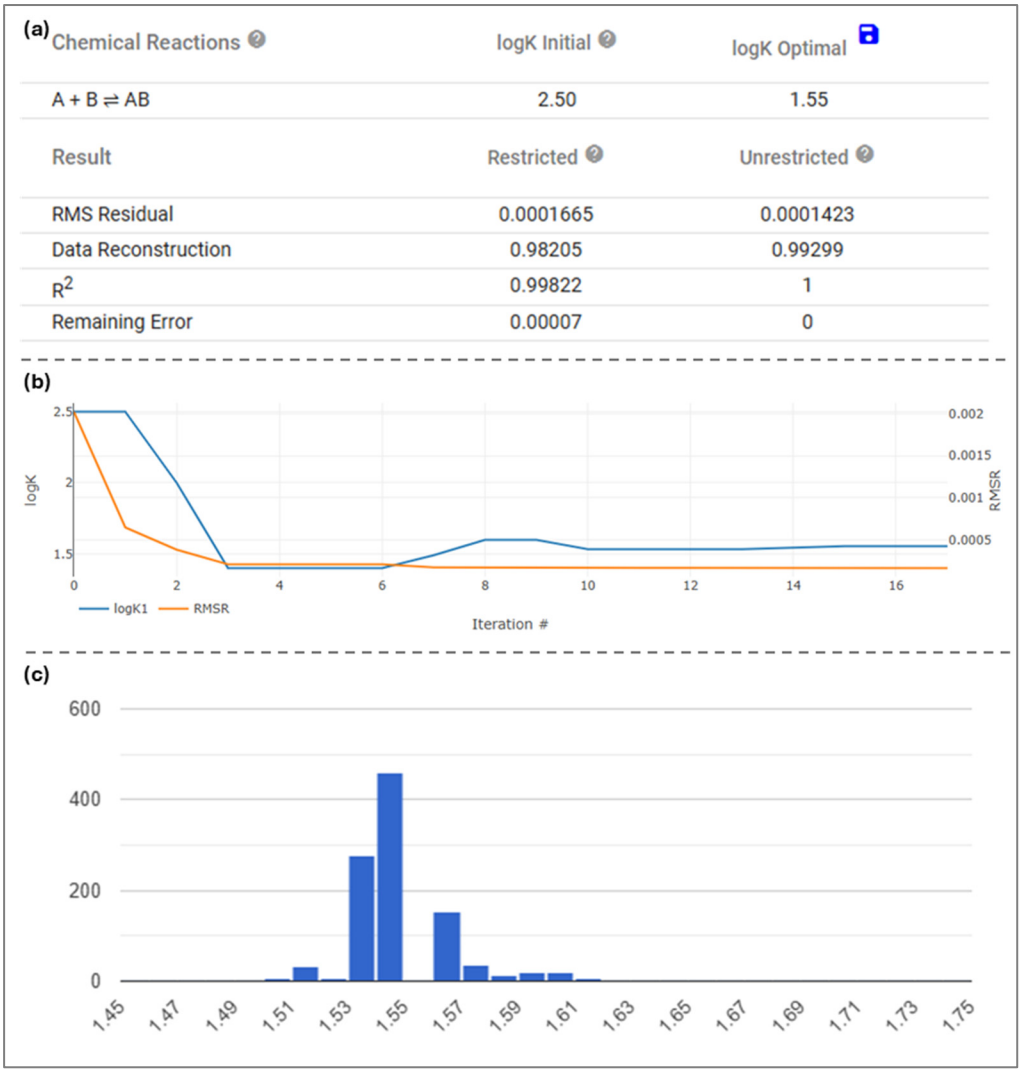

Figure S6. Representative (a) summary table, (b) fitted data, and (c) histogram (1000 bootstraps) for uncertainty analysis for D-IPr·PF_6 (C–N region) and TBACl in dry acetone solution.

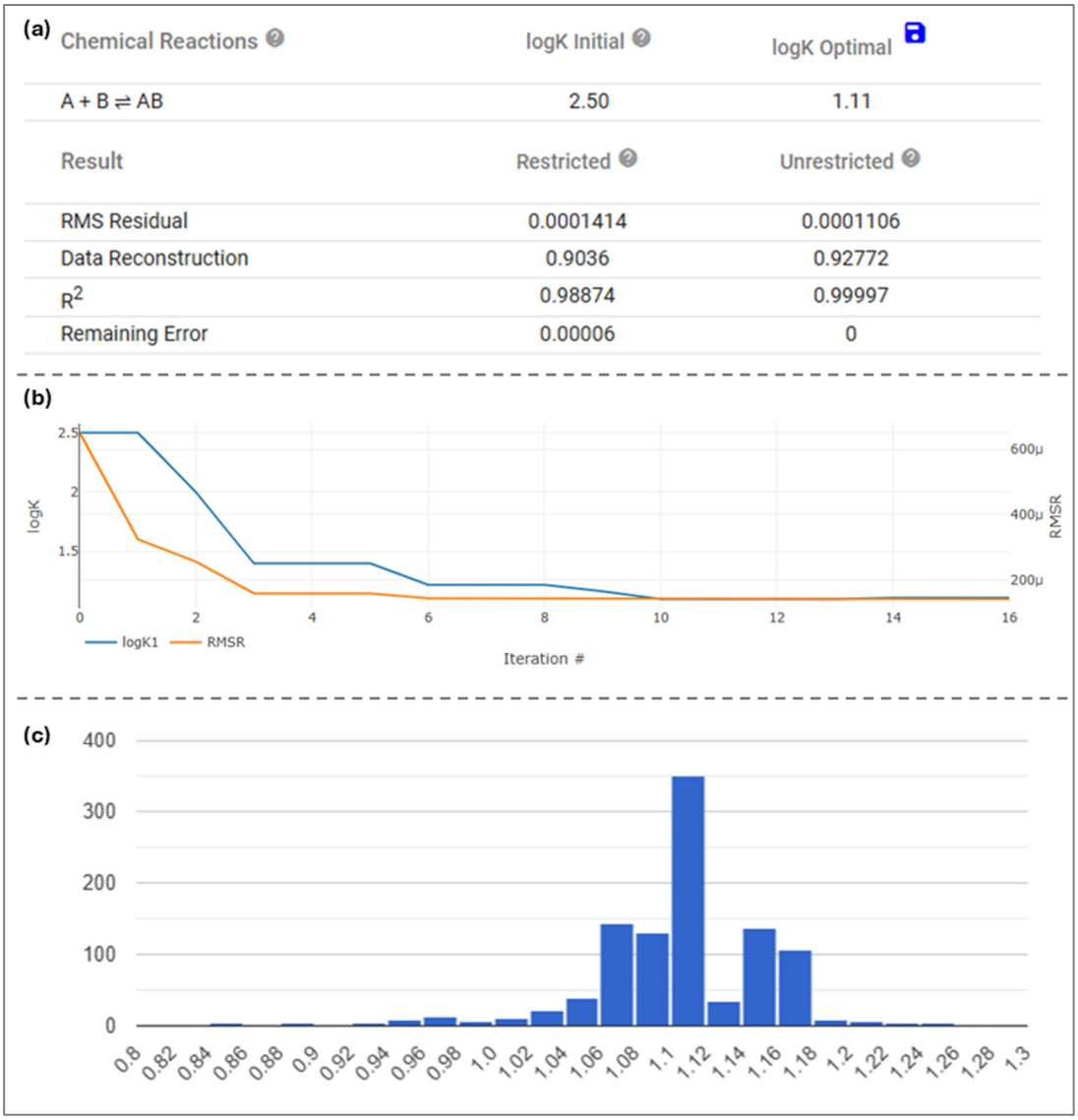

Figure S7. Representative (a) summary table, (b) fitted data, and (c) histogram (1000 bootstraps) for uncertainty analysis for D-IPr·PF_6 (C–D region) (48.3 mM) and TBACl in dry acetone solution.

Table S1. Summary of *in situ* FTIR titration data for D-IPr·PF_6 (48.3 mM) and TBACl in dry acetone solution.

Region	log $K_{1:1}$	95% confidence interval
C–D	1.11	[0.98, 1.17]
C–N	1.55	[1.51, 1.60]

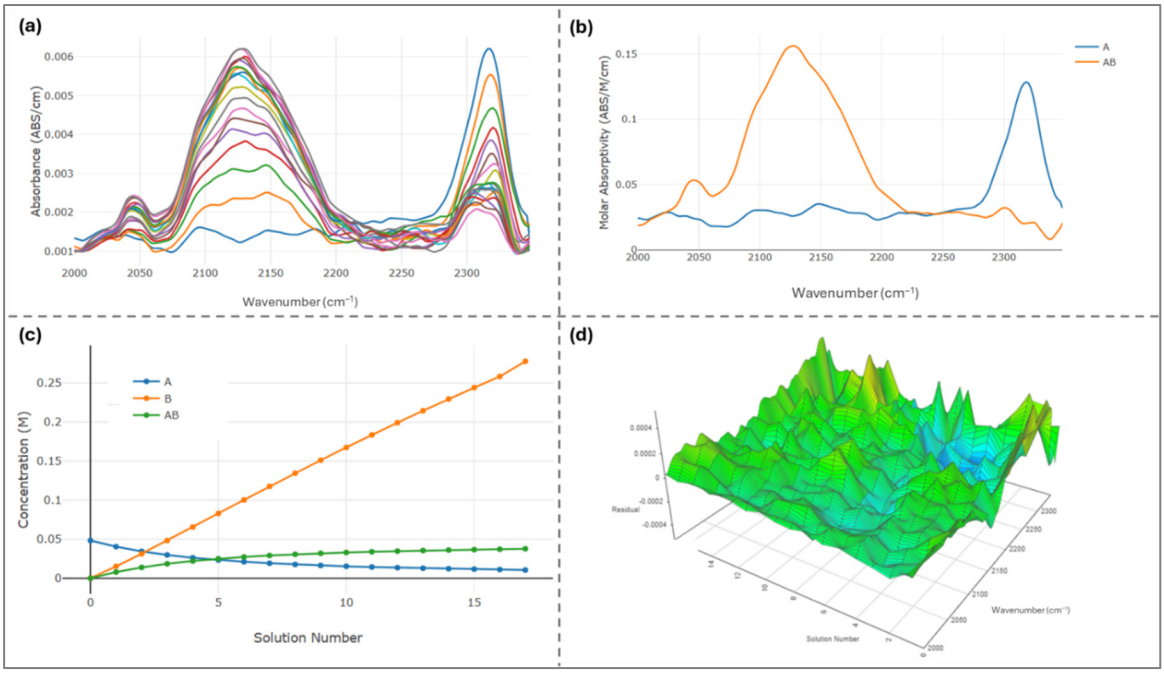

Figure S8. (a) *in situ* FTIR titration spectra of D-IPr·PF_6 (48.3 mM) and TBACl in dry acetone at 298 K. (b) Molar absorptivity plots of the host (blue) and 1:1 host-guest complex (yellow). (c) Concentration data of different host (A, blue), guest (B, yellow), and host-guest complex (AB, green) (d) Residuals obtained from data fitting.

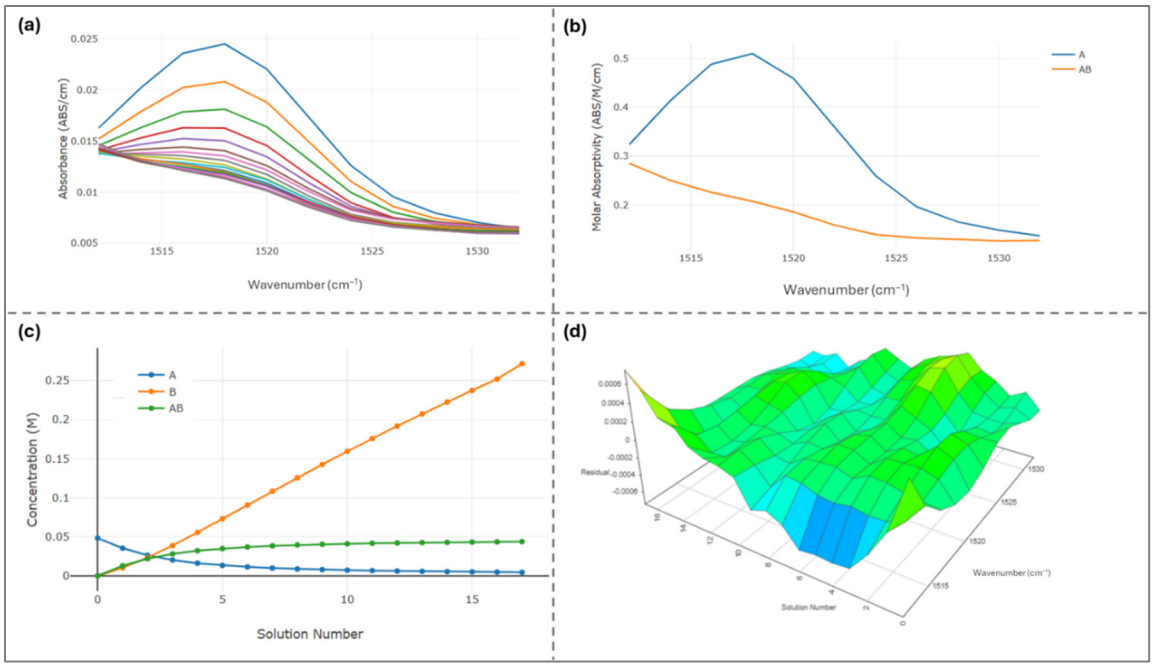

Figure S9. (a) *in situ* FTIR titration spectra of D-IPr·PF_6 (48.3 mM) and TBACl in dry acetone at 298 K. (b) Molar absorptivity plots of the host (blue) and 1:1 host-guest complex (yellow). (c) Concentration data of different host (A, blue), guest (B, yellow), and host-guest complex (AB, green) (d) Residuals obtained from data fitting.

S1.3.2.2 Details and results of *in situ* FTIR titration for H-IPr·PF_6 and TBACl

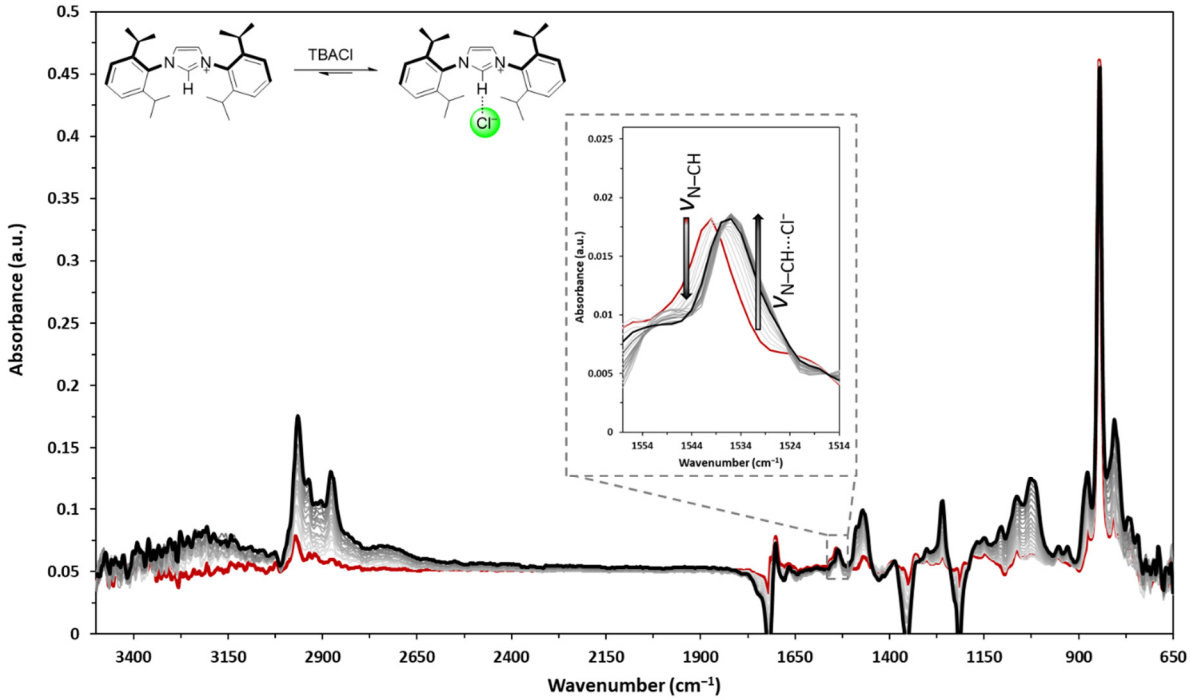

Figure S10. Full *in situ* FTIR titration spectra of H-IPr·PF_6 (48.4 mM) and TBACl in dry acetone at 296 K.

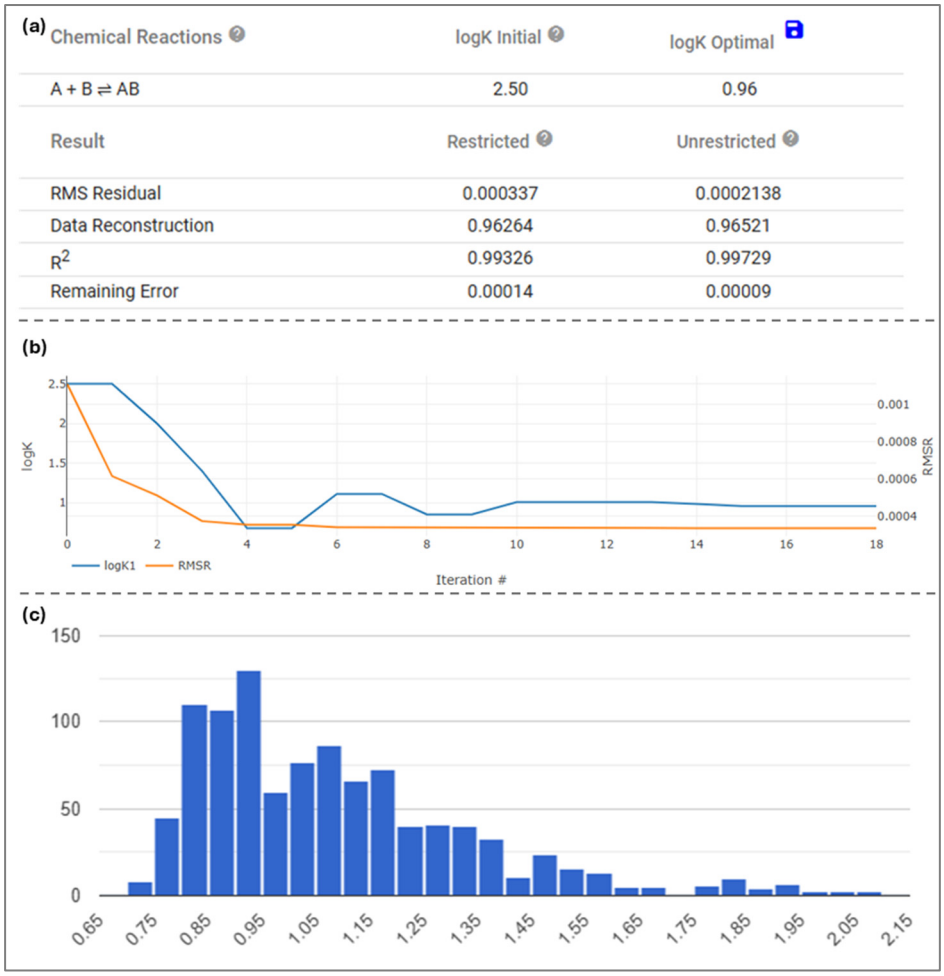

Figure S11. Representative (a) summary table, (b) fitted data, and (c) histogram (1000 bootstraps) for uncertainty analysis for H-IPr·PF_6 (48.4 mM) and TBACl in dry acetone solution.

Table S2. Summary of *in situ* FTIR titration data for H-IPr·PF_6 (48.4 mM) and TBACl in dry acetone solution.

Region	log $K_{1:1}$	95% confidence interval
C–N	0.96	[0.77, 1.76]

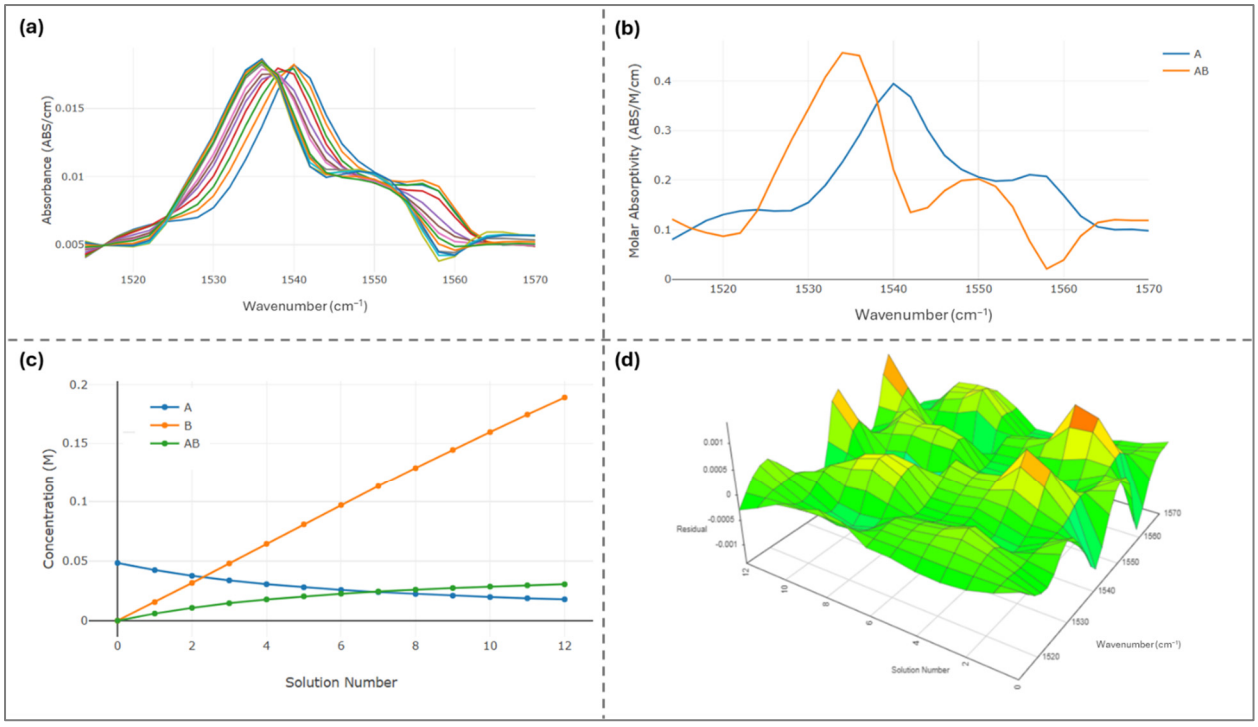

Figure S12. (a) *in situ* FTIR titration spectra of H-IPr·PF_6 (48.4 mM) and TBACl in dry acetone at 298 K. (b) Molar absorptivity plots of the host (blue) and 1:1 host-guest complex (yellow). (c) Concentration data of different host (A, blue), guest (B, yellow), and host-guest complex (AB, green) (d) Residuals obtained from data fitting.

S1.3.2.3 Gaussian deconvolution of the carbonyl region of the *p*-CF_3-tren(*tris*)urea compound

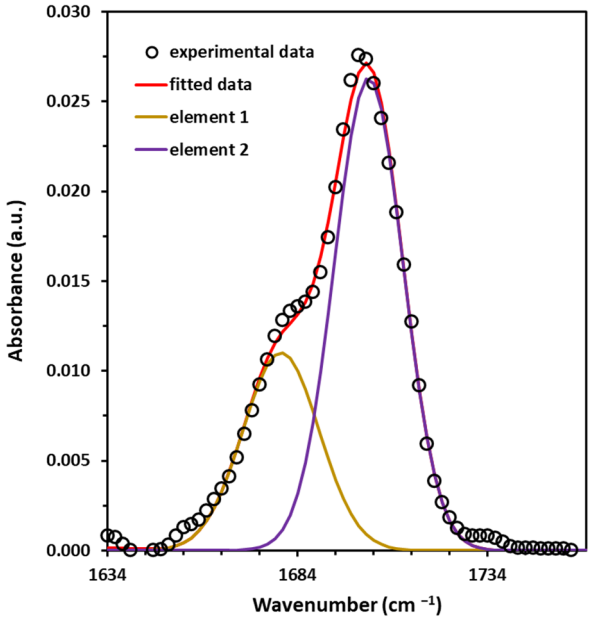

Figure S13. Example of Gaussian deconvolution of the carbonyl region of the *p*-CF_3-tren *(tris)*urea compound. The ratio for the area under the peak of element 1 and element 2 is 46 to 100. Data fitting was performed with the Microsoft Excel package, using the GRG Nonlinear Solving method for 5 elements where the solver found two elements fitting for this solution.

S1.3.2.4 Details and results of *in situ* FTIR titration for *p*-CF_3-tren-*tris*urea and $TBANO_3$

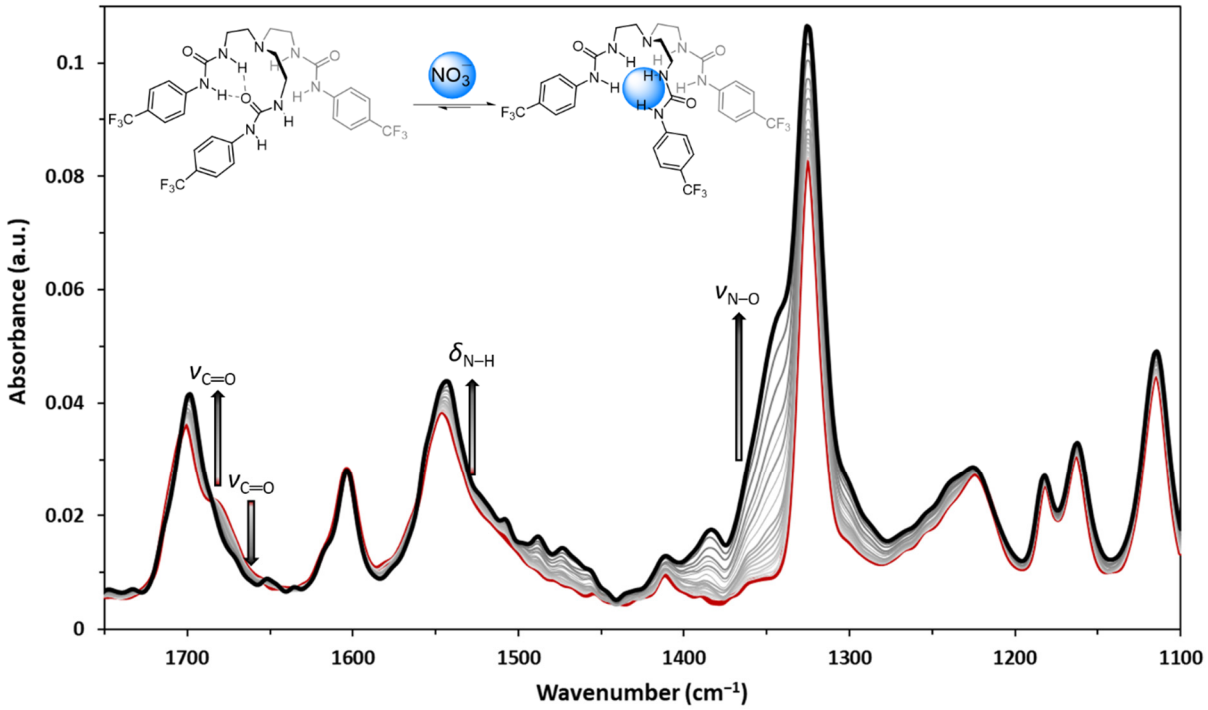

Figure S14. Full *in situ* FTIR titration spectra of *p*-CF_3-tren-*tris*urea (12.7 mM) and $TBANO_3$ in dry 20% DMSO in MeCN solution mixture at 298 K.

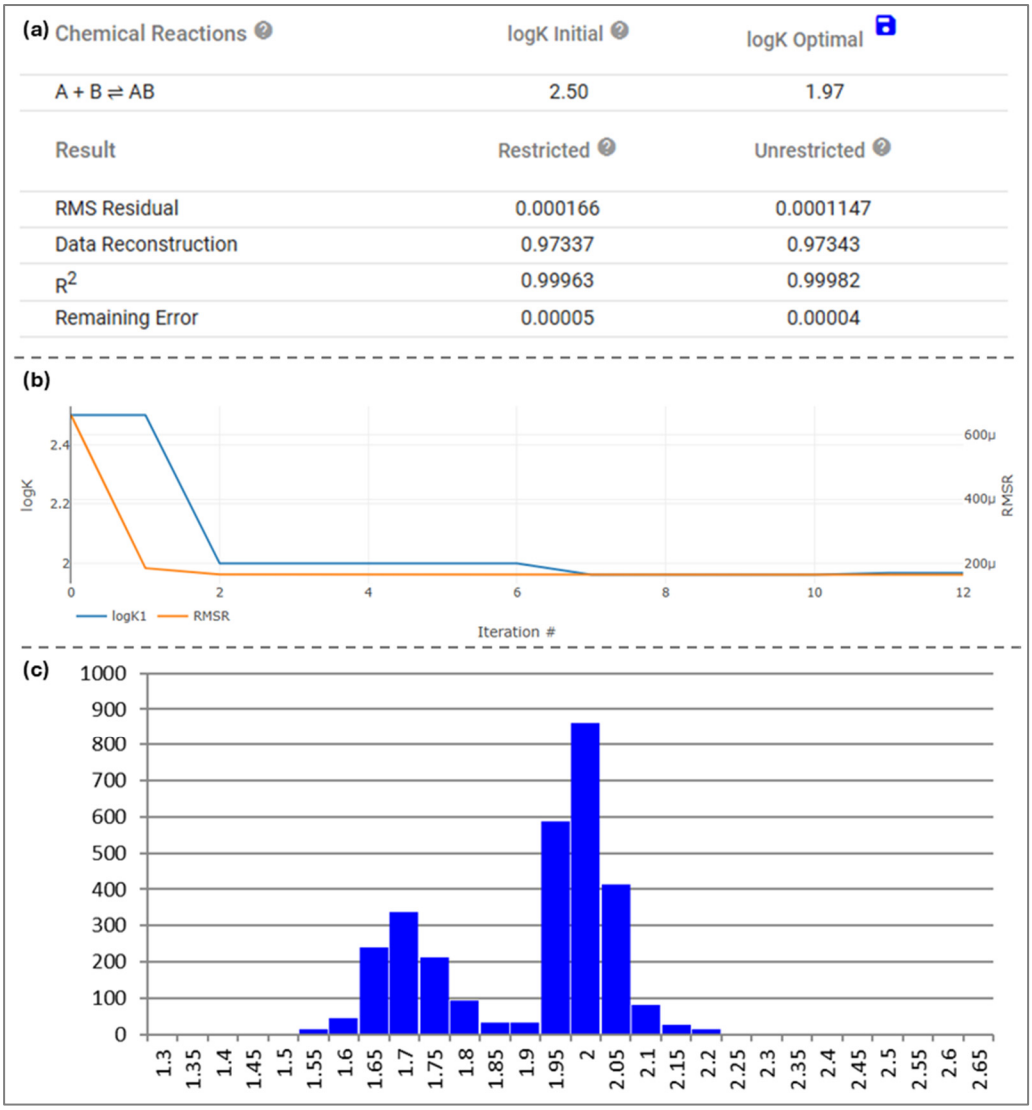

Figure S15. Representative (a) summary table, (b) fitted data, and (c) combined histograms (1000 bootstraps for each trial) for uncertainty analysis for *p*-CF_3-tren-*tris*urea (12.7 mM) and $TBANO_3$ in dry 20% DMSO in MeCN solution.

Table S3. Summary of *in situ* FTIR titration data for *p*-CF_3-tren-*tris*urea (12.7 mM) and $TBANO_3$ in dry 20% DMSO in MeCN solution.

Trial	log $K_{1:1}$	95% confidence interval
1	1.97	[1.91, 2.12]
2	1.96	[1.91, 2.05]
3	1.67	[1.57, 1.85]
Average	1.87	[1.61, 2.08]

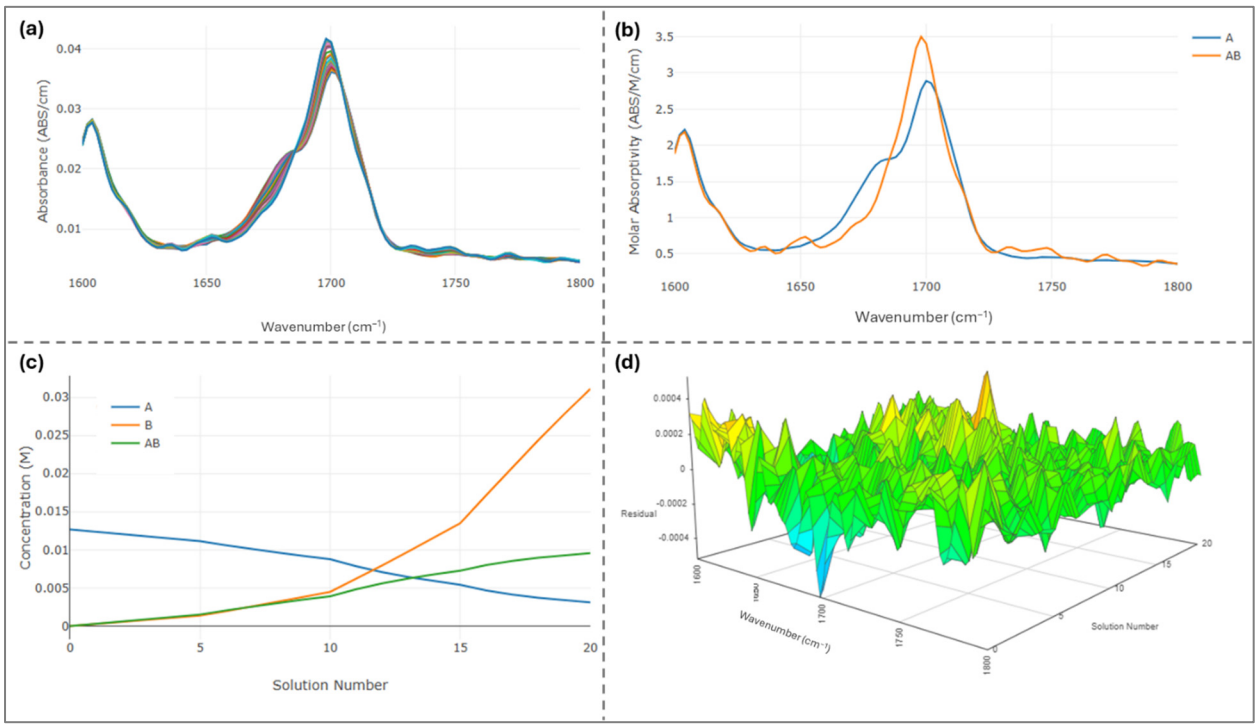

Figure S16. (a) *in situ* FTIR titration spectra of *p*-CF_3-tren-*tris*urea (12.7 mM) and $TBANO_3$ in dry 20% DMSO in MeCN solution mixture at 298 K. (b) Molar absorptivity plots of the host (blue) and 1:1 host-guest complex (yellow). (c) Concentration data of different host (A, blue), guest (B, yellow), and host-guest complex (AB, green) (d) Residuals obtained from data fitting.

S1.3.2.5 Details and results of *in situ* FTIR titration for *p*-CF_3-tren-*tris*urea and $TBAHSO_4$

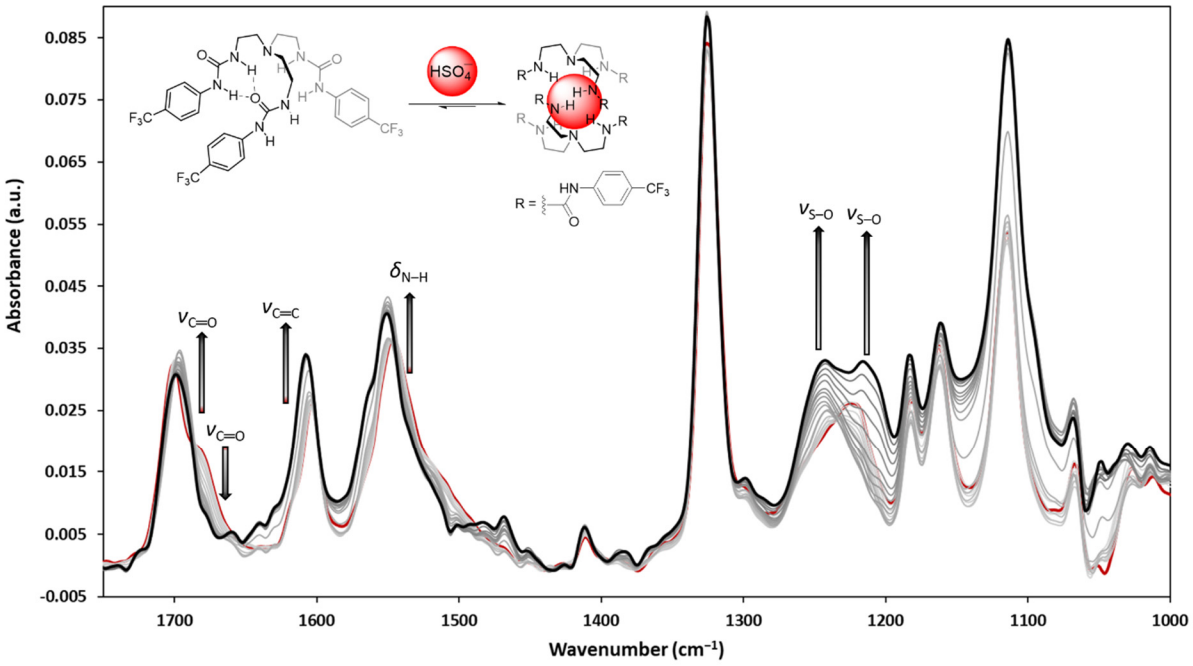

Figure S17. Full *in situ* FTIR titration spectra of *p*-CF_3-tren-*tris*urea (12.5 mM) and $TBAHSO_4$ in dry 20% DMSO in MeCN solution mixture at 298 K.

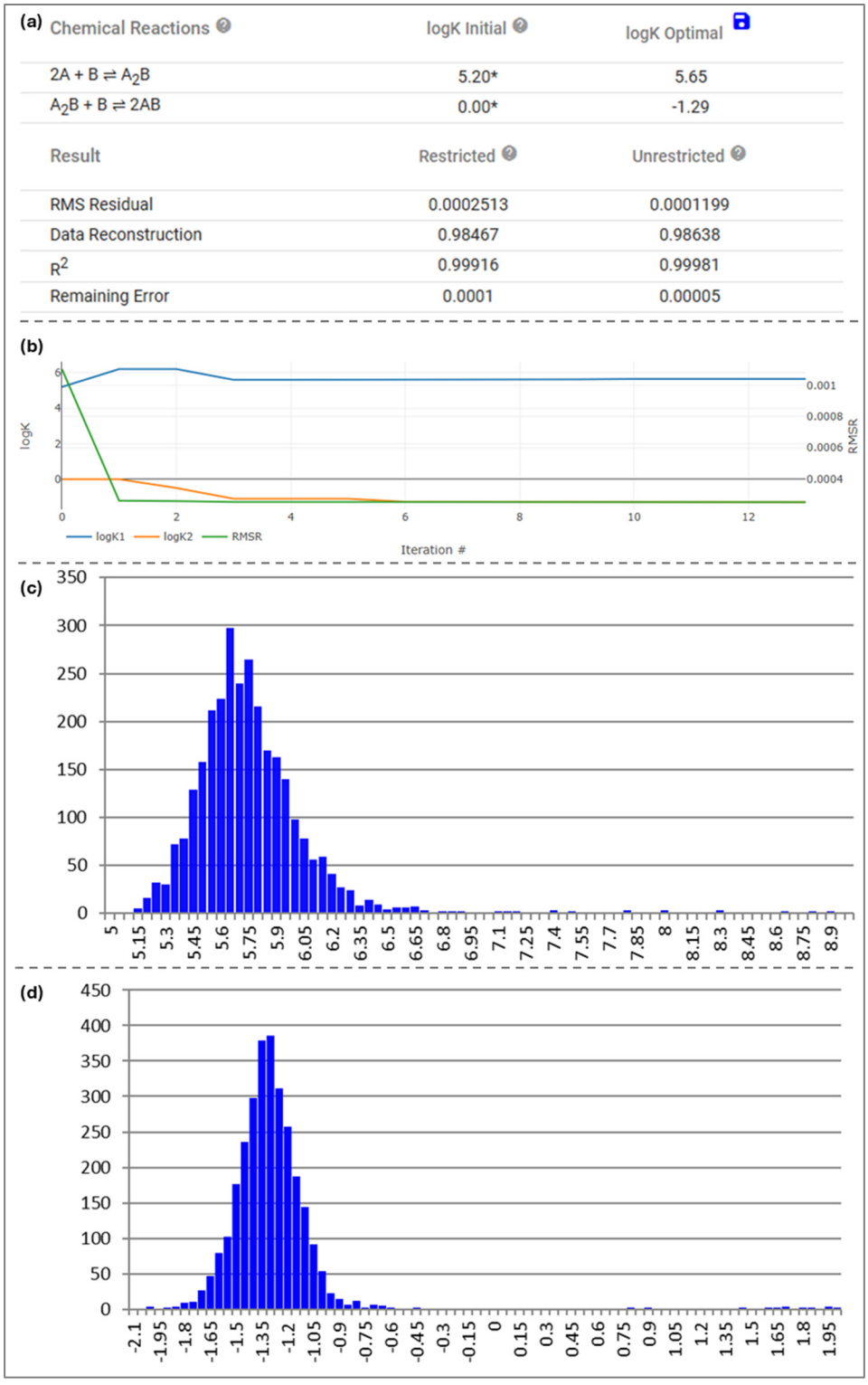

Figure S18. Representative (a) summary table, (b) fitted data, and (c,d) combined histograms (1000 bootstraps for each trial) for uncertainty analysis for $K_{2:1}$ and $K_{1:1}$ (c and d) for *p*-CF_3-tren-*tris*urea (12.5 mM) and $TBAHSO_4$ in dry 20% DMSO in MeCN solution.

Table S4. Summary of *in situ* FTIR titration data for *p*-CF_3-tren-*tris*urea (12.5 mM) and $TBAHSO_4$ in dry 20% DMSO in MeCN solution.

Trial	log $K_{2:1}$	95% confidence interval	log $K_{1:1}$	95% confidence interval
1	5.77	[5.40, 9.31]	−1.40	[−1.72, 2.56]
2	5.78	[5.30, 6.85]	−1.67	[−1.67, 1.78]
3	5.65	[5.24, 8.05]	−1.59	[−1.58, 1.95]
Average	5.73	[5.30, 7.89]	−1.55	[−1.67, 2.04]

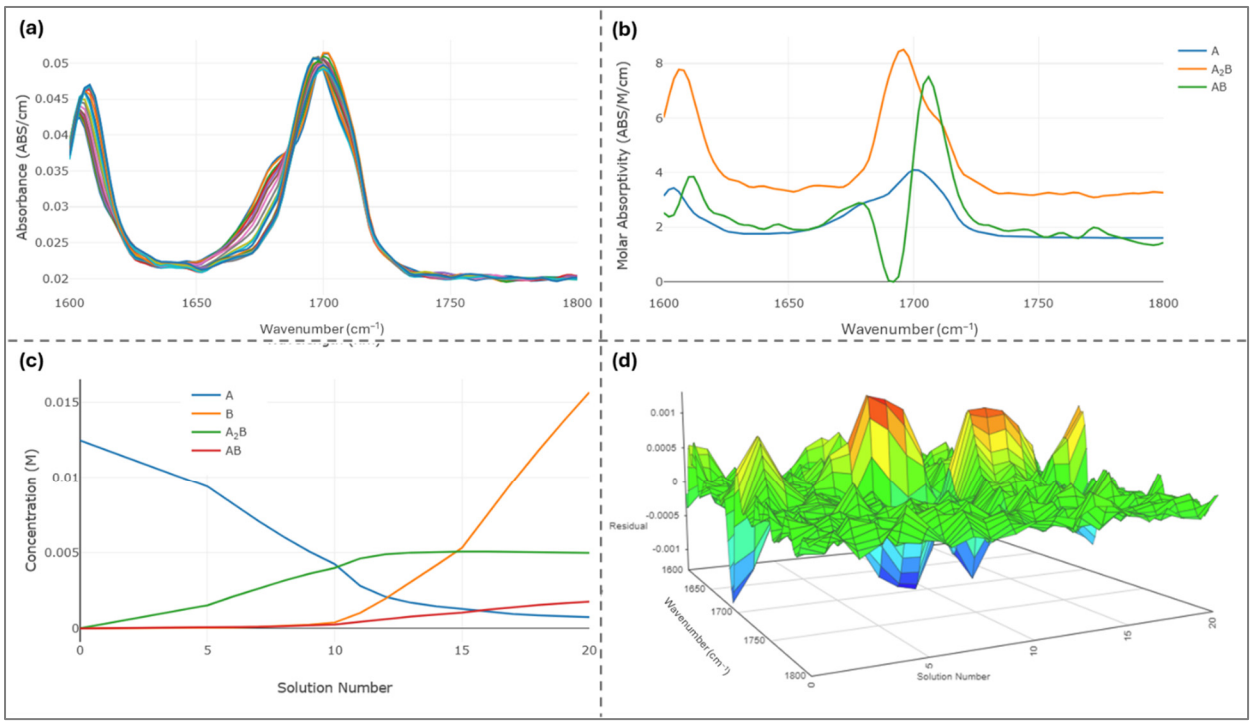

Figure S19. (a) *in situ* FTIR titration spectra of *p*-CF_3-tren (*tris*)urea (12.5 mM) and $TBAHSO_4$ in dry 20% DMSO in MeCN solution mixture at 298 K. (b) Molar absorptivity plots of the host (blue), 2:1 host-guest complex (yellow), and 1:1 host-guest complex (green). (c) Concentration data of different host (A, blue), guest (B, yellow), 2:1 host-guest complex (A_2B, green), and 1:1 host-guest complex (AB, red) (d) Residuals obtained from data fitting.

S1.3.2.6 Details and results of *in situ* FTIR titration for *p*-CF_3-tren-*tris*urea and TBAOCN

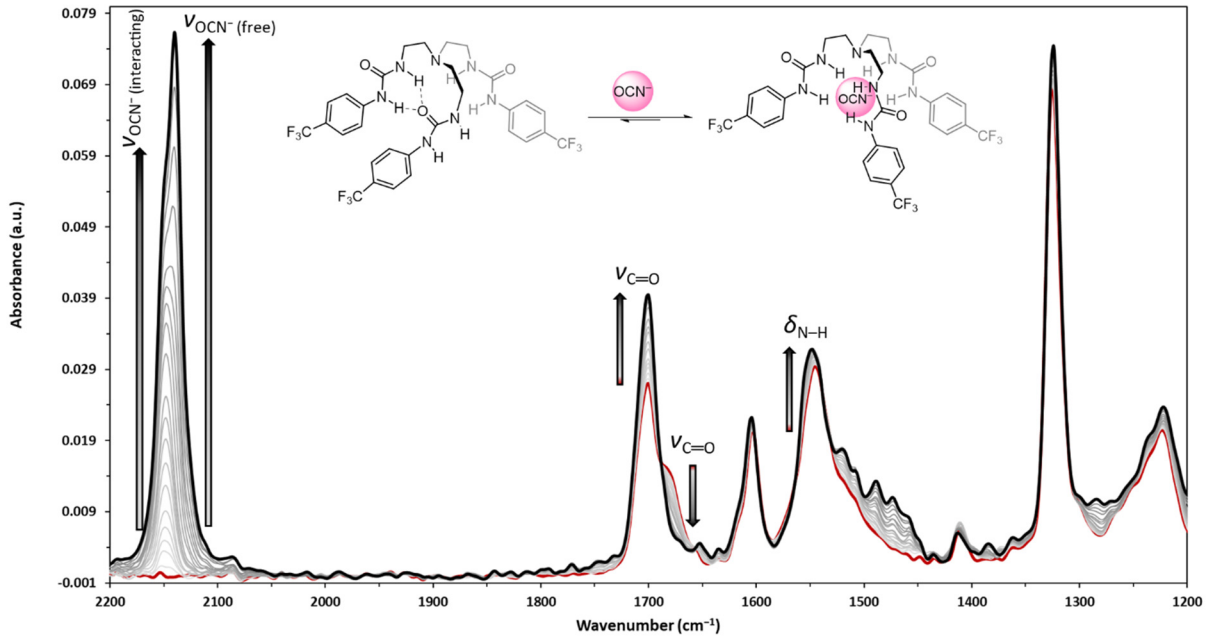

Figure S20. Full *in situ* FTIR titration spectra of *p*-CF_3-tren-*tris*urea (11.6 mM) and TBAOCN in dry 20% DMSO in MeCN solution mixture at 298 K.

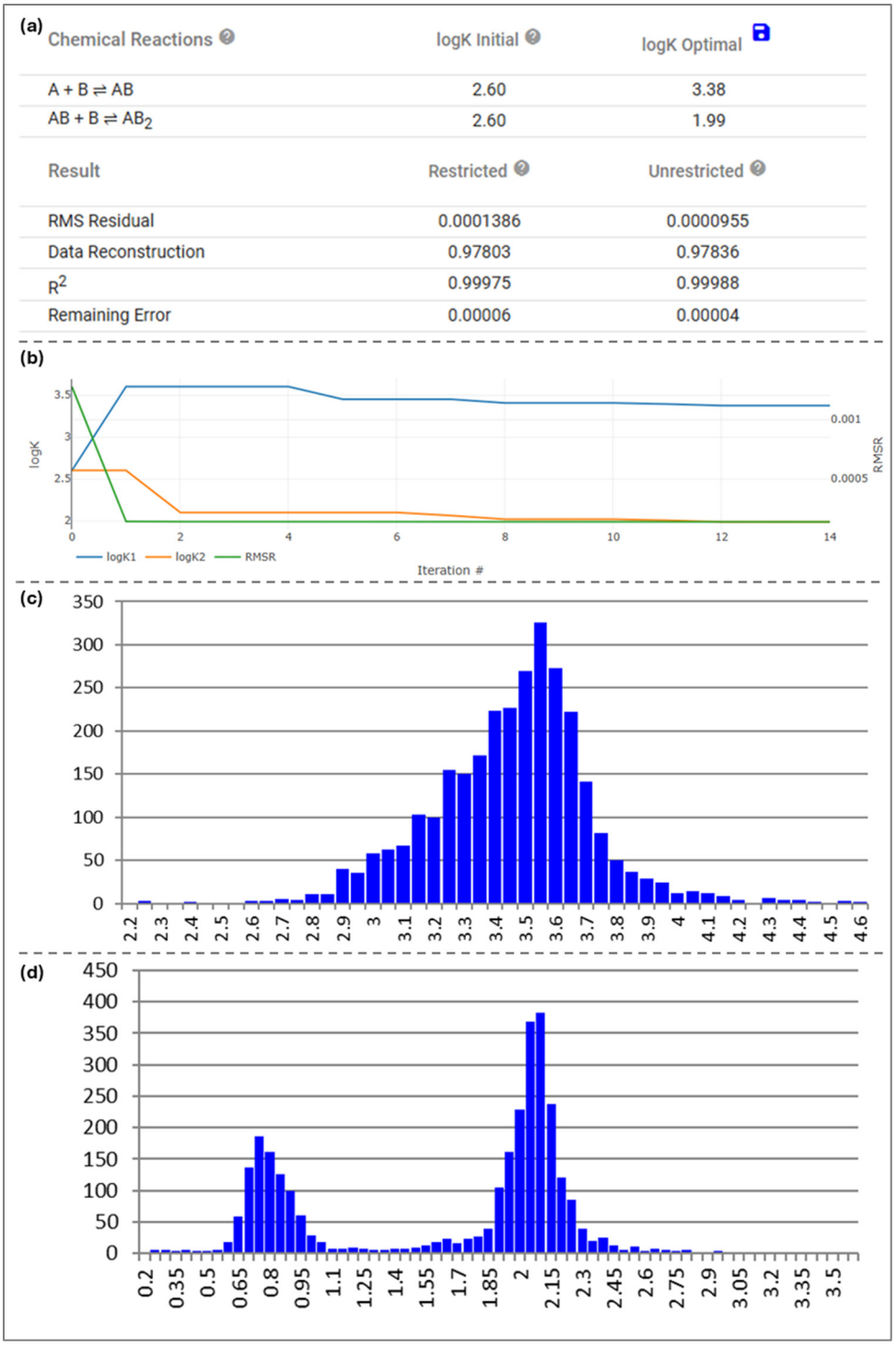

Figure S21. Representative (a) summary table, (b) fitted data, and (c,d) combined histograms (1000 bootstraps for each trial) for uncertainty analysis for $K_{1:1}$ and $K_{1:2}$ (c and d) for *p*-CF_3-tren-*tris*urea (11.6 mM) and TBAOCN in dry 20% DMSO in MeCN solution.

Table S5. Summary of *in situ* FTIR titration data for *p*-CF_3-tren (*tris*)urea (11.6 mM) and TBAOCN in dry 20% DMSO in MeCN solution.

Trial	log $K_{1:1}$	95% confidence interval	log $K_{1:2}$	95% confidence interval
1	3.59	[3.32, 3.92]	0.69	[0.59, 1.79]
2	3.33	[2.94, 3.95]	2.02	[1.98, 2.55]
3	3.38	[2.80, 4.33]	1.99	[0.67, 2.28]
Average	3.43	[2.90, 4.13]	1.57	[0.63, 2.41]

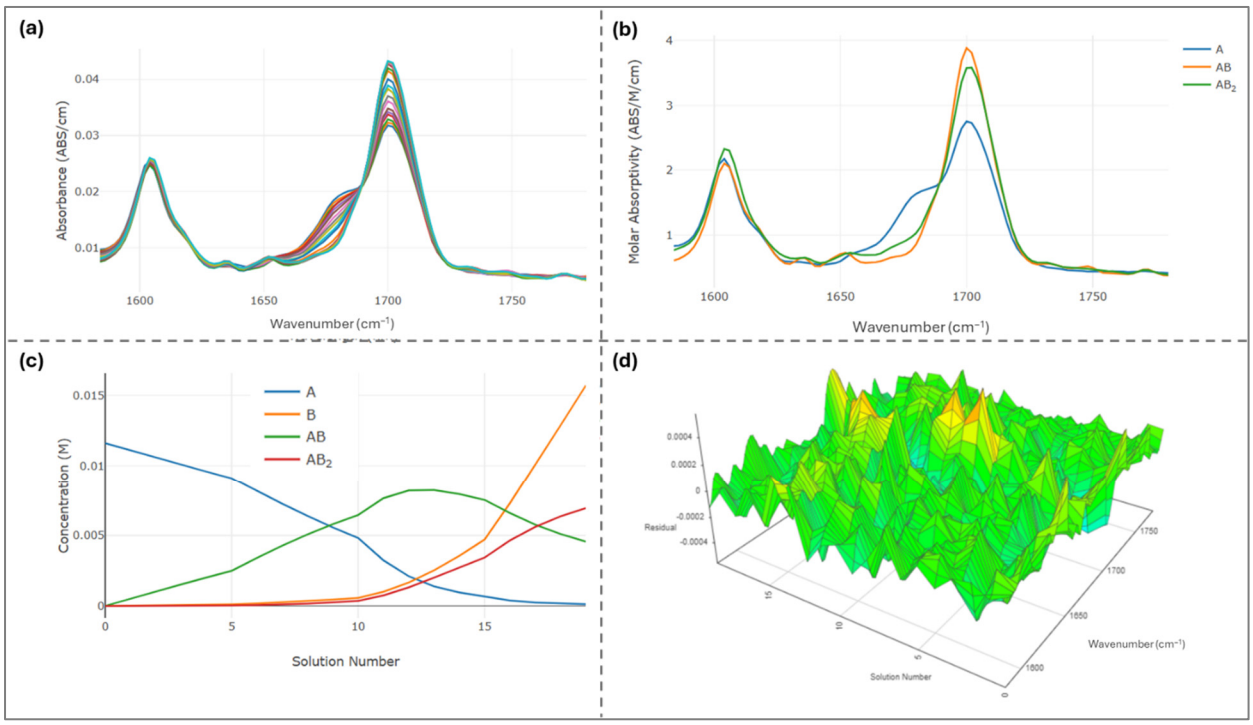

Figure S22. (a) *in situ* FTIR titration spectra of *p*-CF_3-tren-*tris*urea (11.6 mM) and TBAOCN in dry 20% DMSO in MeCN solution at 298 K. (b) Molar absorptivity plots of the host (blue), 1:1 host-guest complex (yellow), and 1:2 host-guest complex (green). (c) Concentration data of different host (A, blue), guest (B, yellow), 1:1 host-guest complex (AB, green), and 1:2 host-guest complex (AB_2, red) (d) Residuals obtained from data fitting.

S1.3.2.7 Details and results of *in situ* FTIR titration for TBAOCN and *p*-CF_3-tren-*tris*urea

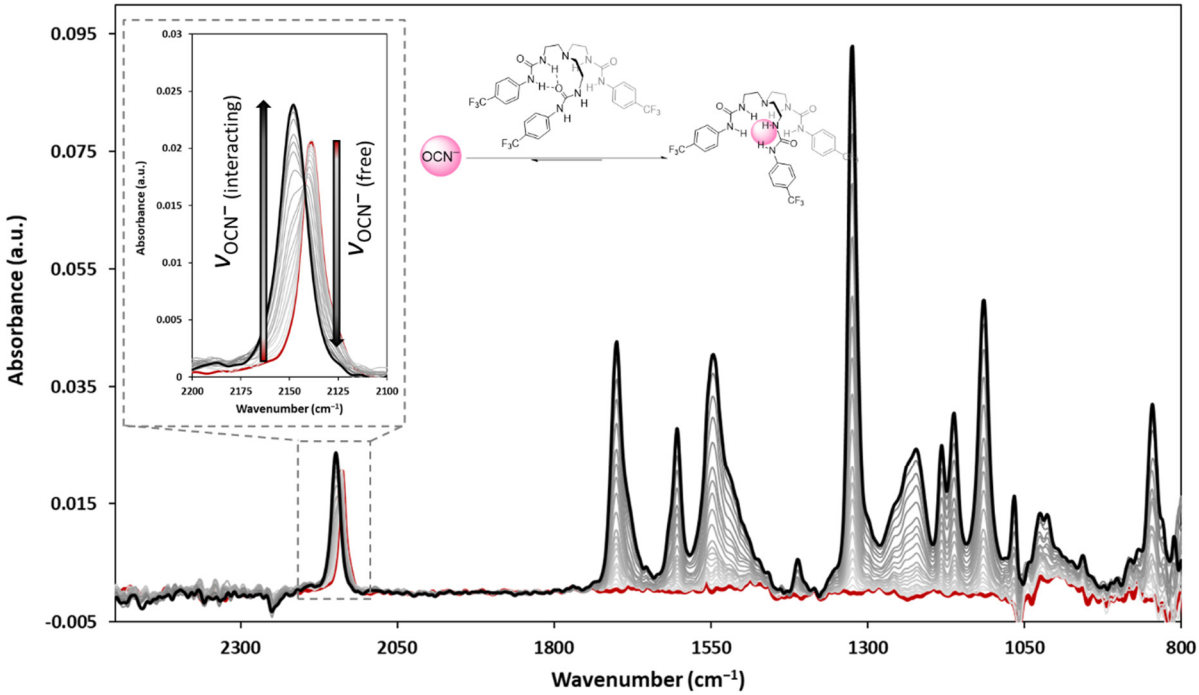

Figure S23. Full *in situ* FTIR titration spectra of TBAOCN (6.67 mM) and *p*-CF_3-tren-*tris*urea in dry 20% DMSO in MeCN solution mixture at 298 K.

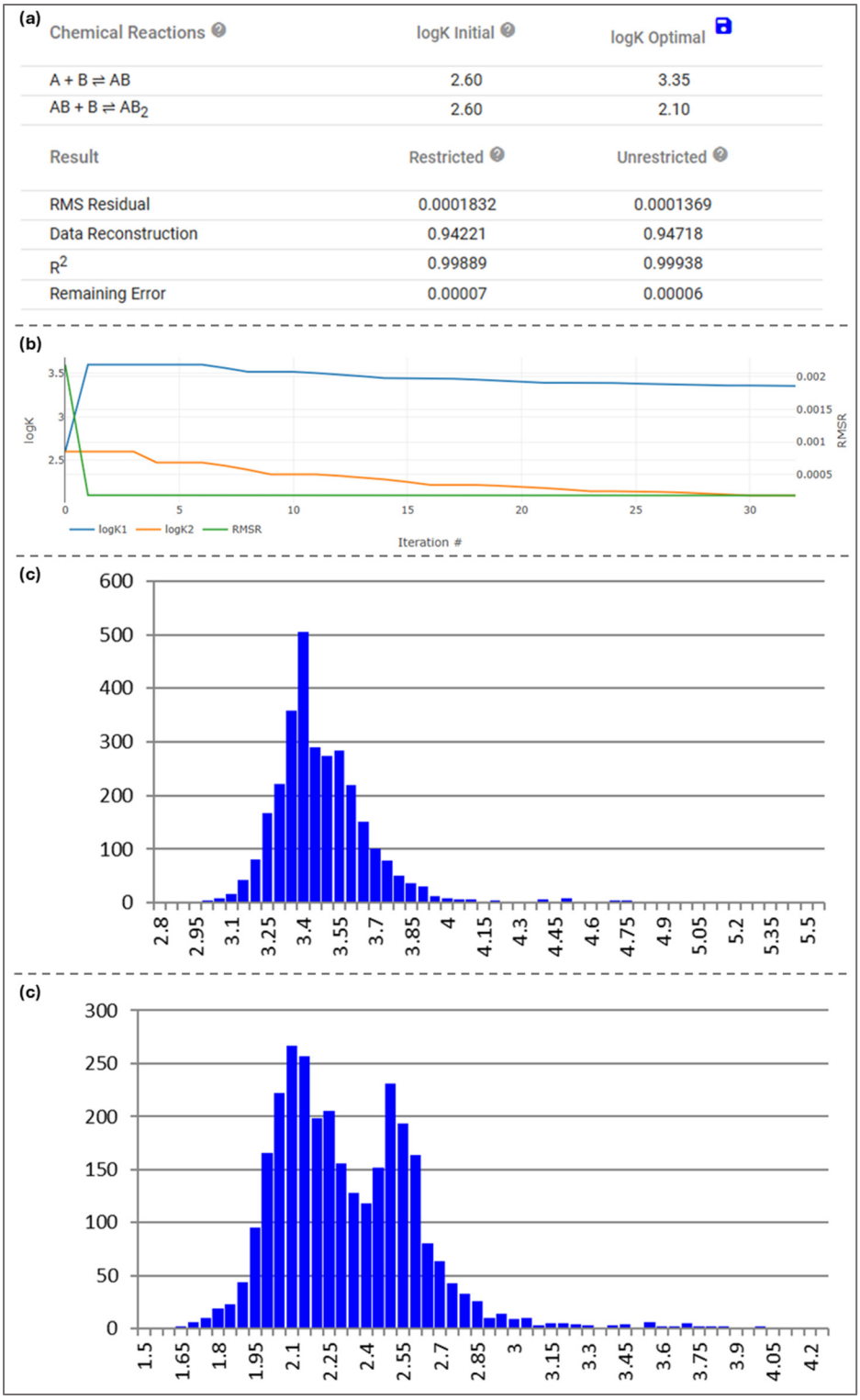

Figure S24. Representative (a) summary table, (b) fitted data, and (c) combined histograms (1000 bootstraps for each trial) uncertainty analysis for $K_{1:1}$ and $K_{1:2}$ (c and d) for TBAOCN and *p*-CF_3-tren-*tris*urea (6.67 mM) in dry 20% DMSO in MeCN solution.

Table S6. Summary of *in situ* FTIR titration data for TBAOCN and *p*-CF_3-tren-*tris*urea (6.67 mM) in dry 20% DMSO in MeCN solution.

Trial	log $K_{1:1}$	95% confidence interval	log $K_{1:2}$	95% confidence interval
1	3.36	[3.11, 3.95]	2.10	[1.85, 2.83]
2	3.51	[3.16, 3.87]	2.04	[1.83, 2.55]
3	3.37	[3.22, 4.03]	2.51	[2.37, 3.17]
Average	3.41	[3.16, 3.94]	2.22	[1.87, 2.95]

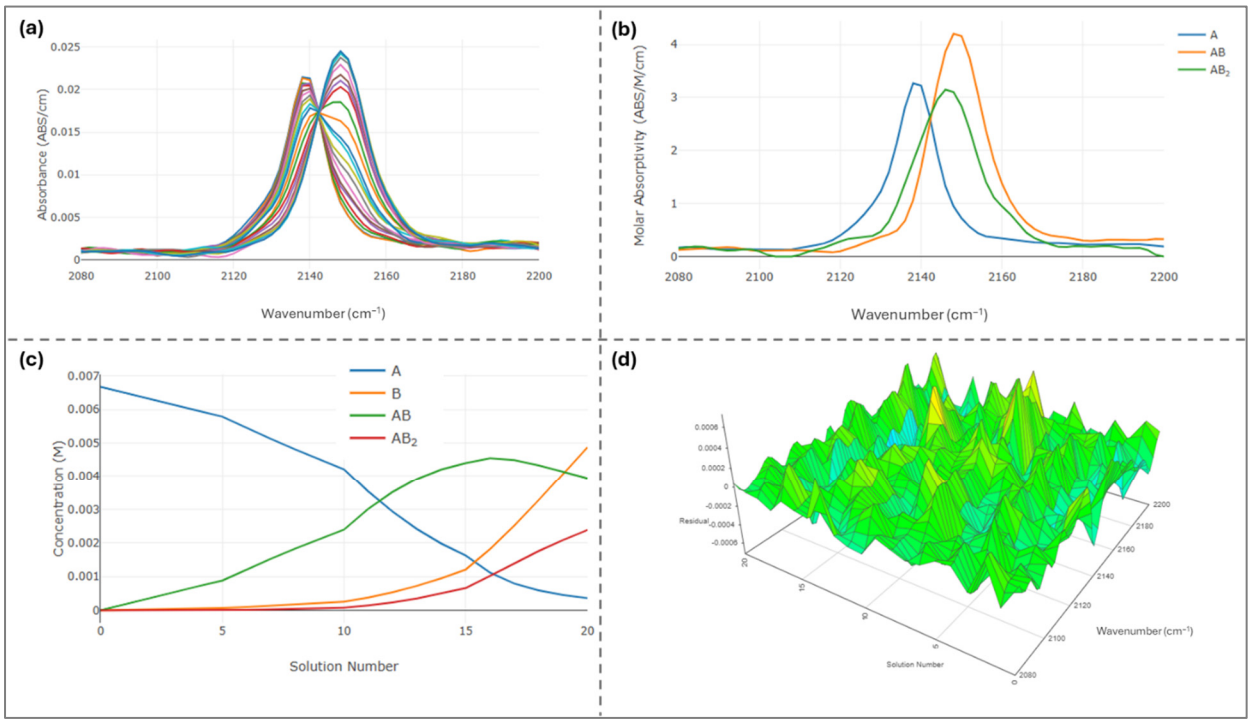

Figure S25. (a) *in situ* FTIR titration spectra of TBAOCN (6.67 mM) and *p*-CF_3-tren-*tris*urea in dry 20% DMSO in MeCN solution at 298 K. (b) Molar absorptivity plots of the host (blue), 1:1 host-guest complex (yellow), and 1:2 host-guest complex (green). (c) Concentration data of different host (A, blue), guest (B, yellow), 1:1 host-guest complex (AB, green), and 1:2 host-guest complex (AB_2, red) (d) Residuals obtained from data fitting.

S1.3.2.8 Details and results of *in situ* FTIR titration for NBS and TBACl

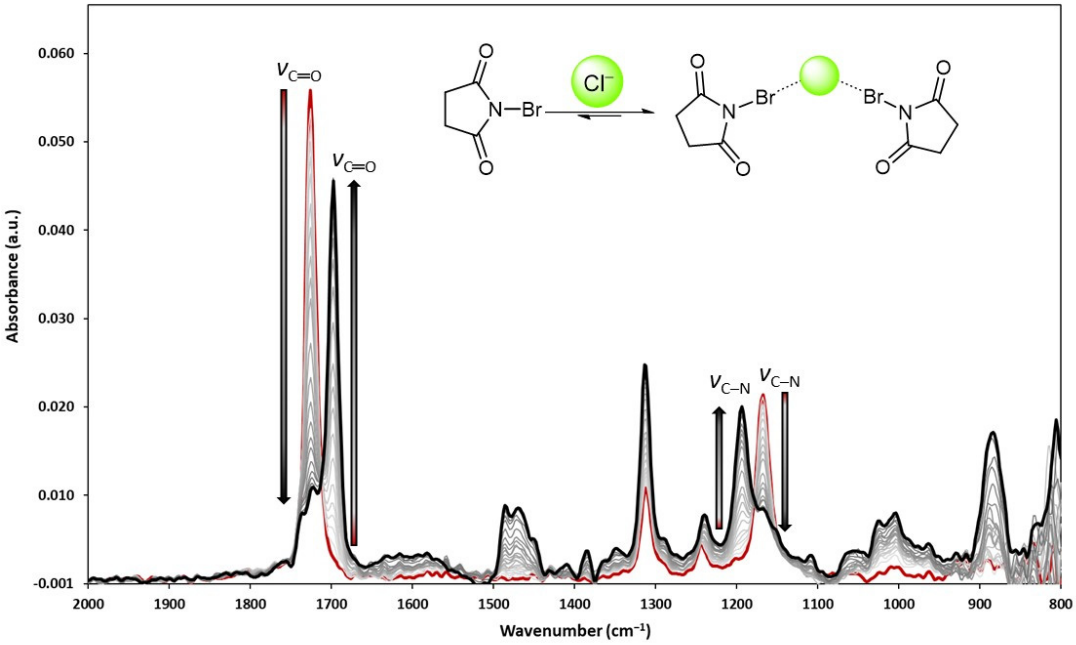

Figure S26. Full *in situ* FTIR titration spectra of NBS (20.3 mM) and TBACl in MeCN solution at 298 K.

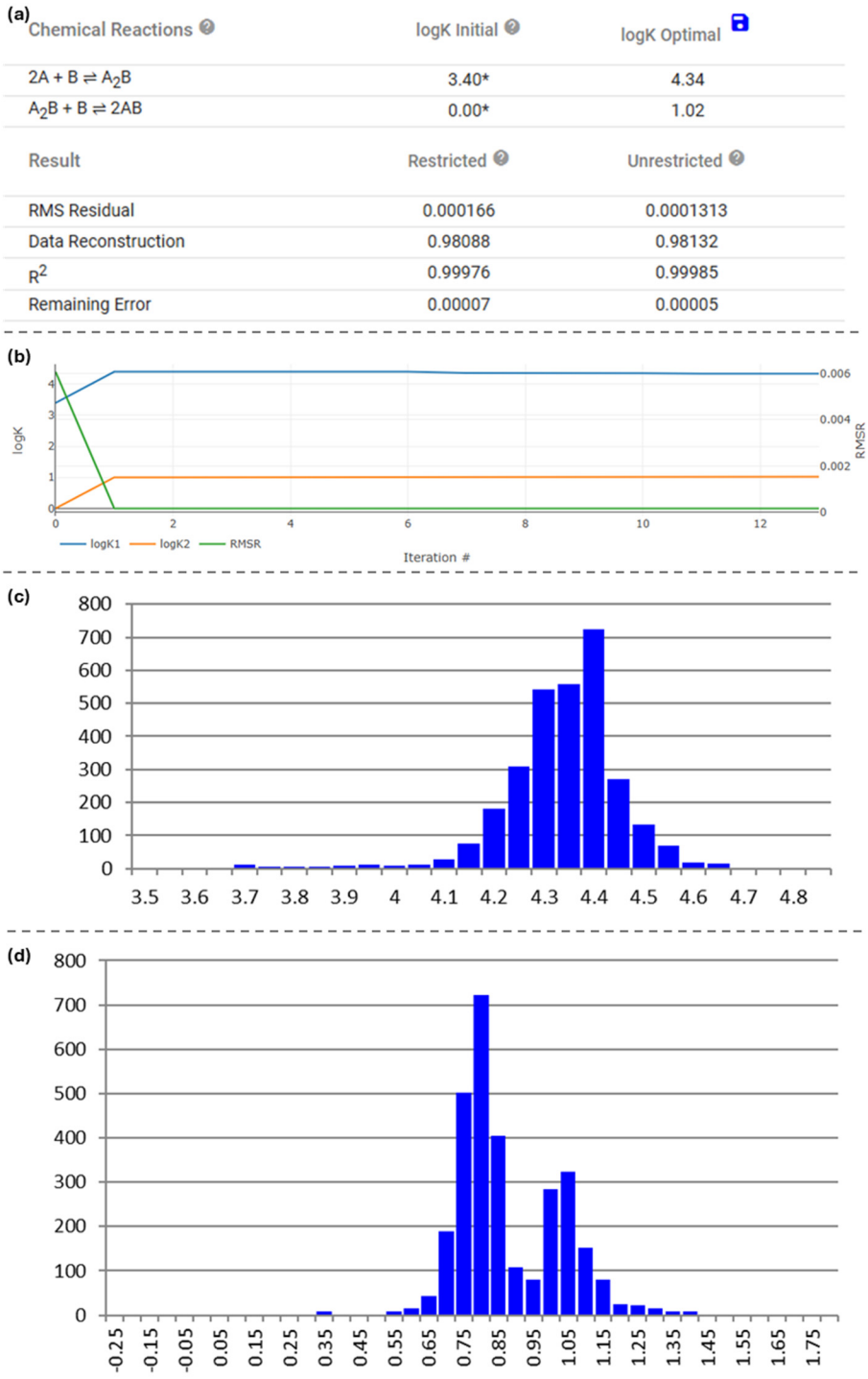

Figure S27. Representative (a) summary table, (b) fitted data, and (c) combined histograms (1000 bootstraps for each trial) for uncertainty analysis for $K_{2:1}$ and $K_{1:1}$ (c and d) for NBS (20.3 mM) and TBACl in MeCN solution.

Table S7. Summary of *in situ* FTIR titration data for NBS (20.3 mM) and TBACl in MeCN solution.

Trial	log $K_{2:1}$	95% confidence interval	log $K_{1:1}$	95% confidence interval
1	4.39	[3.89, 4.51]	1.00	[0.88, 1.26]
2	4.27	[4.15, 4.53]	0.90	[0.88, 0.98]
3	4.56	[4.18, 4.56]	0.78	[0.63, 0.94]
Average	4.41	[4.07, 4.53]	0.89	[0.65, 1.16]

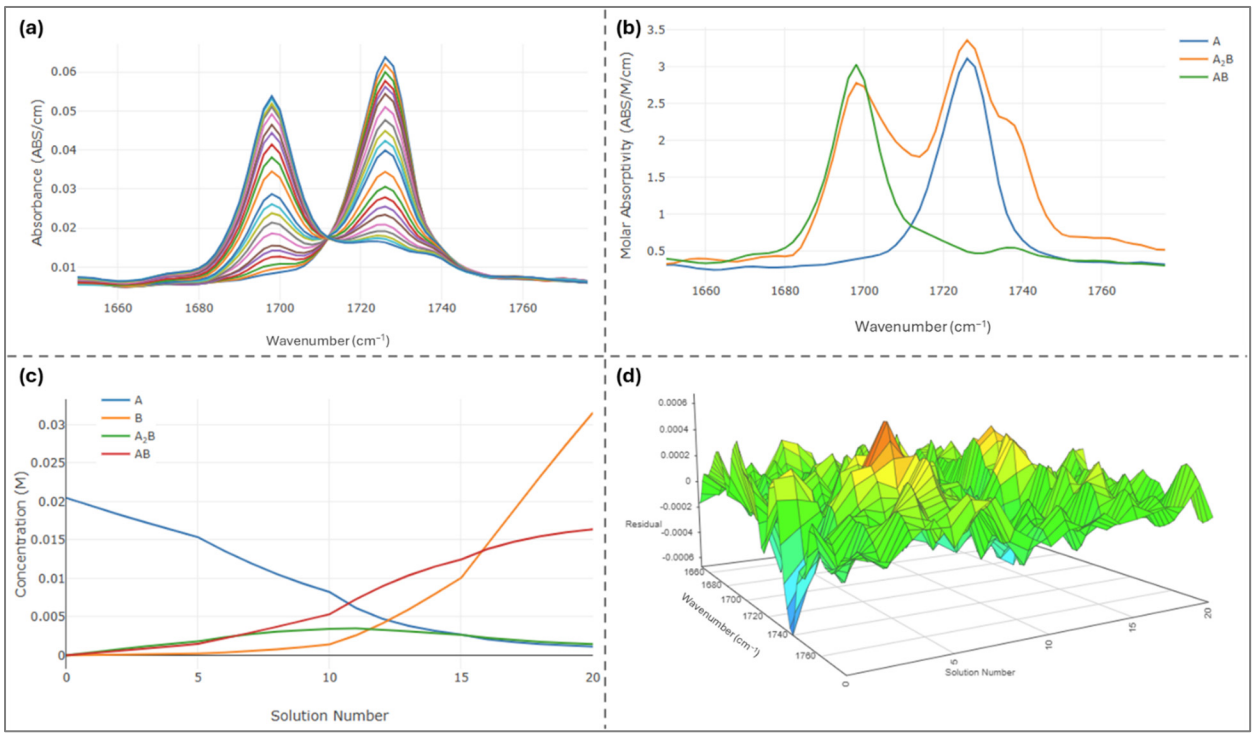

Figure S28. (a) *in situ* FTIR titration spectra of NBS (20.3 mM) and TBACl in MeCN solution at 298 K. (b) Molar absorptivity plots of the host (blue), 2:1 host-guest complex (yellow), and 1:1 host-guest complex (green). (c) Concentration data of different host (A, blue), guest (B, yellow), 2:1 host-guest complex (A_2B, green), and 1:1 host-guest complex (AB, red) (d) Residuals obtained from data fitting.

S1.3.2.9 Details and results of *in situ* FTIR titration for NBS and TBABr

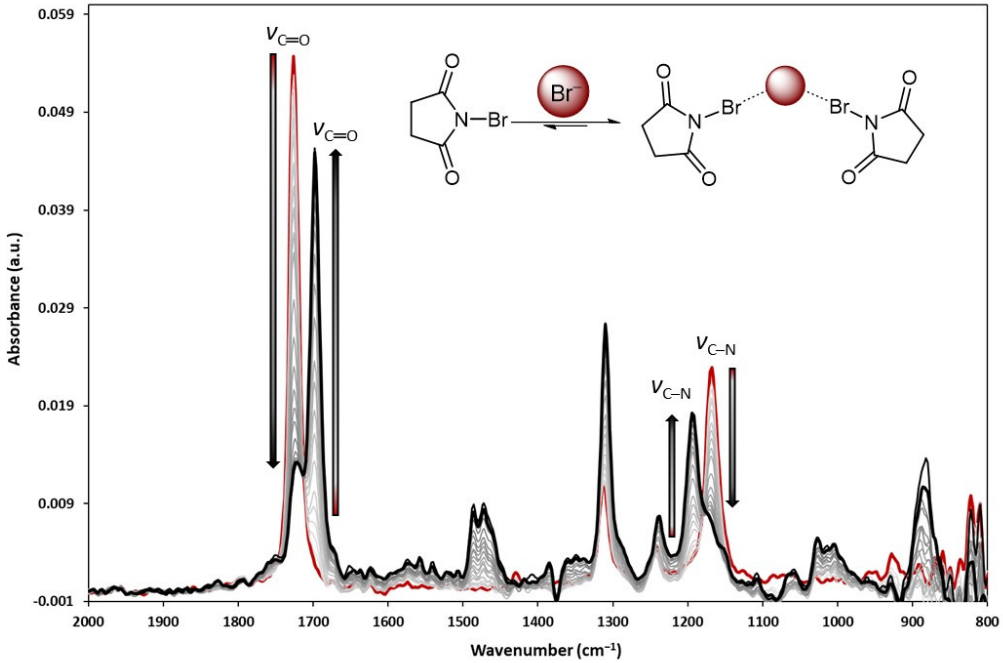

Figure S29. Full *in situ* FTIR titration spectra of NBS (18.2 mM) and TBABr in MeCN solution at 298 K.

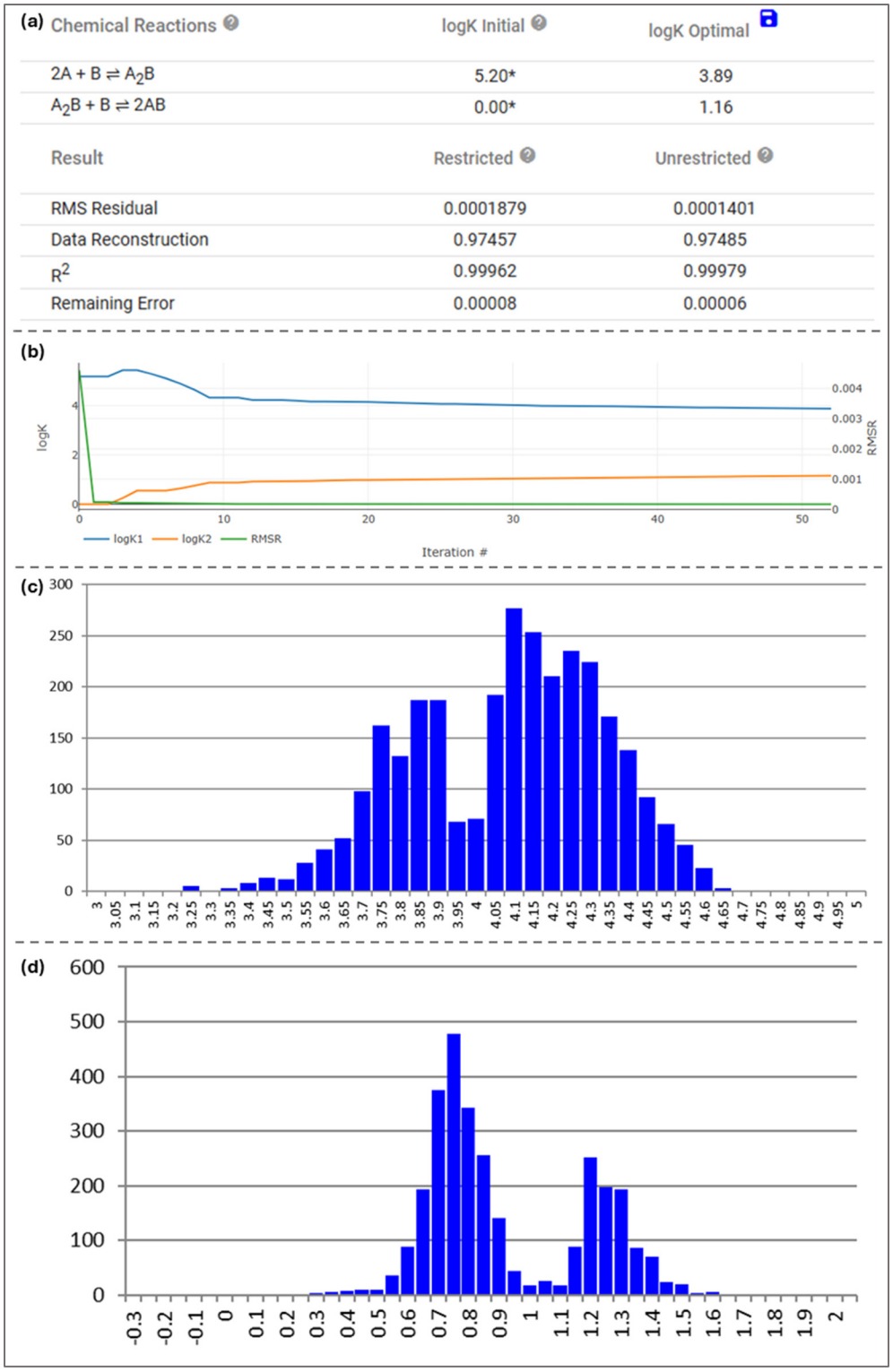

Figure S30. Representative (a) summary table, (b) fitted data, and (c) combined histograms (1000 bootstraps for each trial) for uncertainty analysis for $K_{2:1}$ and $K_{1:1}$ (c and d) for NBS (18.2mM) and TBABr in MeCN solution.

Table S8. Summary of *in situ* FTIR titration data for NBS (18.2 mM) and TBABr in MeCN solution.

Trial	log $K_{2:1}$	95% confidence interval	log $K_{1:1}$	95% confidence interval
1	4.13	[3.95, 4.13]	0.78	[0.54, 0.91]
2	4.27	[3.99, 4.56]	0.73	[0.48, 0.90]
3	3.89	[3.44, 3.96]	1.16	[1.03, 1.46]
Average	4.10	[3.68, 4.49]	0.89	[0.55, 1.38]

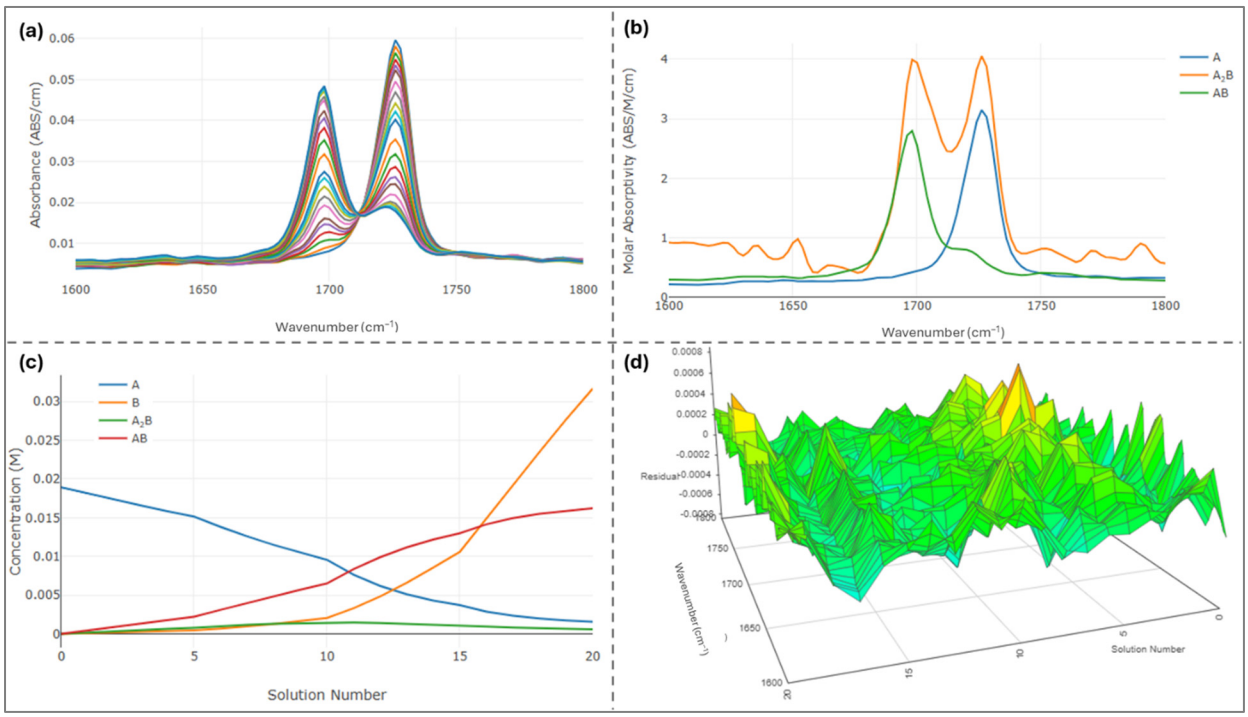

Figure S31. (a) *in situ* FTIR titration spectra of NBS (18.2 mM) and TBABr in MeCN solution at 298 K. (b) Molar absorptivity plots of the host (blue), 2:1 host-guest complex (yellow), and 1:1 host-guest complex (green). (c) Concentration data of different host (A, blue), guest (B, yellow), 2:1 host-guest complex (A_2B, green), and 1:1 host-guest complex (AB, red) (d) Residuals obtained from data fitting.

S1.3.3 ^{1}H NMR titrations

All NMR titrations were collected at 25 °C on a Varian Inova-500 instrument. All chemical shifts (δ) are reported in ppm relative to residue CHD_2CN (^{1}H: 1.940 ppm) or acetone-d_6 (^{1}H: 2.05 ppm). Stock solutions of the receptor D/H-IPr·PF_6 and *p*-CF_3-tren (*tris*)urea were prepared in either dry acetone-d_6 or 20%DMSO-d_6 in MeCN-d_3. To maintain a constant host concentration during the course of the titration, each guest was dissolved in 2 mL of the host solution at the desired concentrations and transferred to septum-sealed vials.[5] The host stock solution (500 μL) was added to three separate NMR tubes equipped with septum-sealed screw caps. After the collection of a background ^{1}H NMR spectrum, an aliquot of the TBAX solution was added to the NMR tube using a gas-tight syringe, and the resultant ^{1}H NMR spectrum was recorded. Titration data were fit using parametric equilibrium-restricted global analysis (PERGA) using the SIVVU program.[6] Different fitting models were tested to confirm the best fit from each set of data. Titrations were performed in triplicate, and the final values reported in each table are the average of K_a and the histogram of combined 95% confidence intervals for the three titrations.[7]

S1.3.3.1 Details and results of ^{1}H NMR titration for D-IPr·PF_6 (1.4 mM) and TBACl **Table S9**. Representative titration data of D-IPr·PF_6 (1.4 mM) with Cl^-.

	V guest (µL)	equiv. guest	[host] (M)	[guest] (M)	δ1 (ppm)	δ2 (ppm)	δ3 (ppm)
1	0	0.00	0.00137	0.000	8.4568	7.7135	7.5664
2	2	0.29	0.00137	0.000396	8.4516	7.7076	7.5603
3	4	0.58	0.00137	0.000788	8.4493	7.7045	7.5569
4	6	0.86	0.00137	0.00118	8.4460	7.7002	7.5525
5	8	1.14	0.00137	0.00156	8.4428	7.6961	7.5484
6	10	1.42	0.00137	0.00195	8.4410	7.6936	7.5459
7	12	1.70	0.00137	0.00233	8.4384	7.6903	7.5425
8	14	1.98	0.00137	0.00270	8.4380	7.6891	7.5413
9	16	2.25	0.00137	0.00308	8.4356	7.6861	7.5383
10	18	2.52	0.00137	0.00345	8.4353	7.6852	7.5372
11	20	2.79	0.00137	0.00382	8.4325	7.6821	7.5339
12	25	3.45	0.00137	0.00473	8.4307	7.6791	7.5309
13	30	4.11	0.00137	0.00562	8.4292	7.6762	7.5280
14	40	5.37	0.00137	0.00736	8.4262	7.6709	7.5224
15	50	6.59	0.00137	0.00903	8.4240	7.6662	7.5176
16	100	12.09	0.00137	0.0165	8.4211	7.6557	7.5063

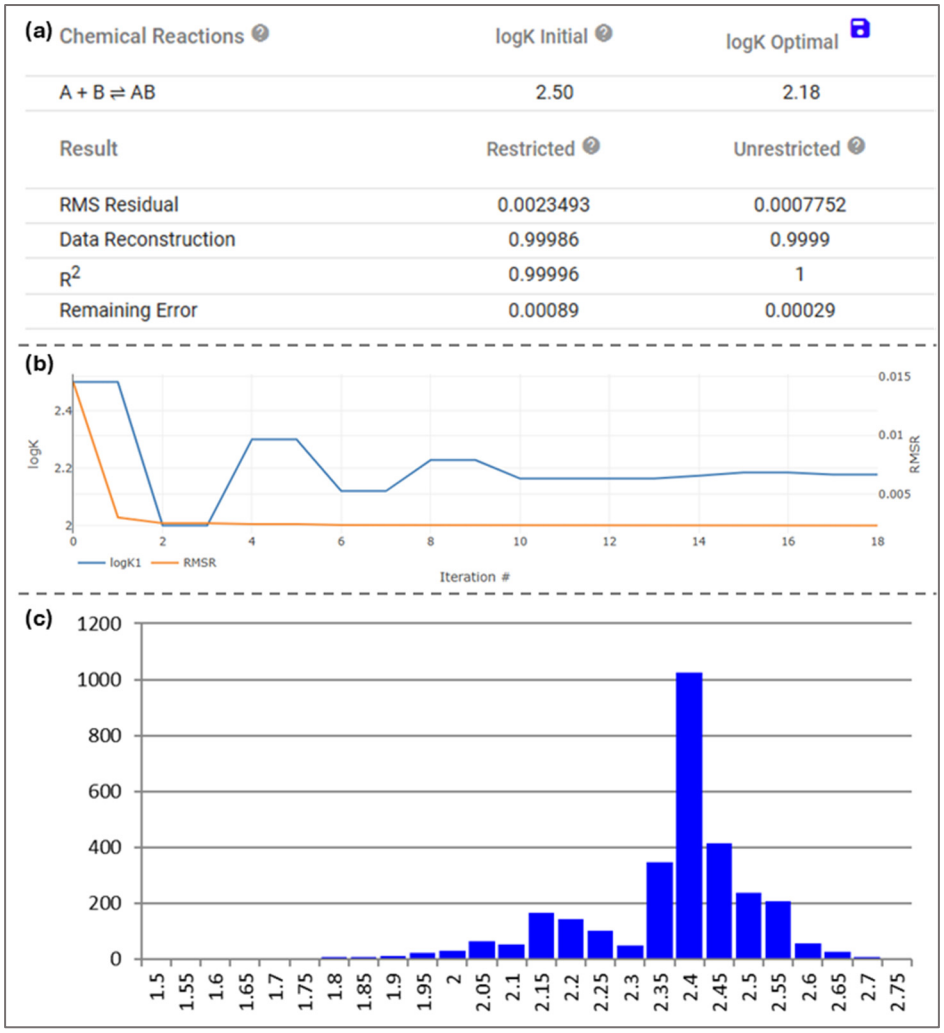

Figure S32. Representative (a) summary table, (b) fitted data, and (c) combined histograms (1000 bootstraps for each trial) for uncertainty analysis for D-IPr·PF_6 (1.4 mM) with Cl^- in dry acetone-d_6.

Table S10. Summary of ^{1}H NMR titration data for D-IPr·PF_6 (1.4 mM) and TBACl in dry acetone-d_6.

Trial	log $K_{1:1}$	95% confidence interval
1	2.44	[2.30, 2.51]
2	2.18	[1.85, 2.62]
3	2.38	[2.32, 2.52]
Average	2.33	[1.97, 2.56]

S1.3.3.2 Details and results of ^{1}H NMR titration for H-IPr·PF_6 (1.3 mM) and TBACl

Table S11. Representative titration data of H-IPr·PF_6 (1.3 mM) with Cl^-.

	V guest (µL)	equiv. guest	[host] (M)	[guest] (M)	δ1 (ppm)	δ2 (ppm)	δ3 (ppm)
1	0	0.00	0.00127	0.000	9.8213	8.4586	7.7140
2	2	0.38	0.00127	0.000487	10.0454	8.4488	7.7053
3	4	0.76	0.00127	0.00097	10.2172	8.4426	7.6998
4	6	1.14	0.00127	0.001451	10.3473	8.4371	7.6948
5	8	1.51	0.00127	0.00193	10.4550	8.4336	7.6911
6	10	1.89	0.00127	0.00240	10.5547	8.4289	7.6870
7	12	2.25	0.00127	0.00287	10.6313	8.4245	7.6824
8	14	2.62	0.00127	0.00333	10.7004	8.4224	7.6808
9	16	2.98	0.00127	0.00379	10.7688	8.4214	7.6794
10	18	3.34	0.00127	0.00425	10.8080	8.4180	7.6762
11	20	3.70	0.00127	0.00470	10.8671	8.4158	7.6737
12	25	4.58	0.00127	0.00583	10.9748	8.4134	7.6708
13	40	7.12	0.00127	0.00906	11.2158	8.4063	7.6619
14	50	8.74	0.00127	0.0111	11.3272	8.4045	7.6586
15	100	16.03	0.00127	0.0204	11.6147	8.4005	7.6469
16	150	22.19	0.00127	0.0282	11.7835	8.4010	7.6397

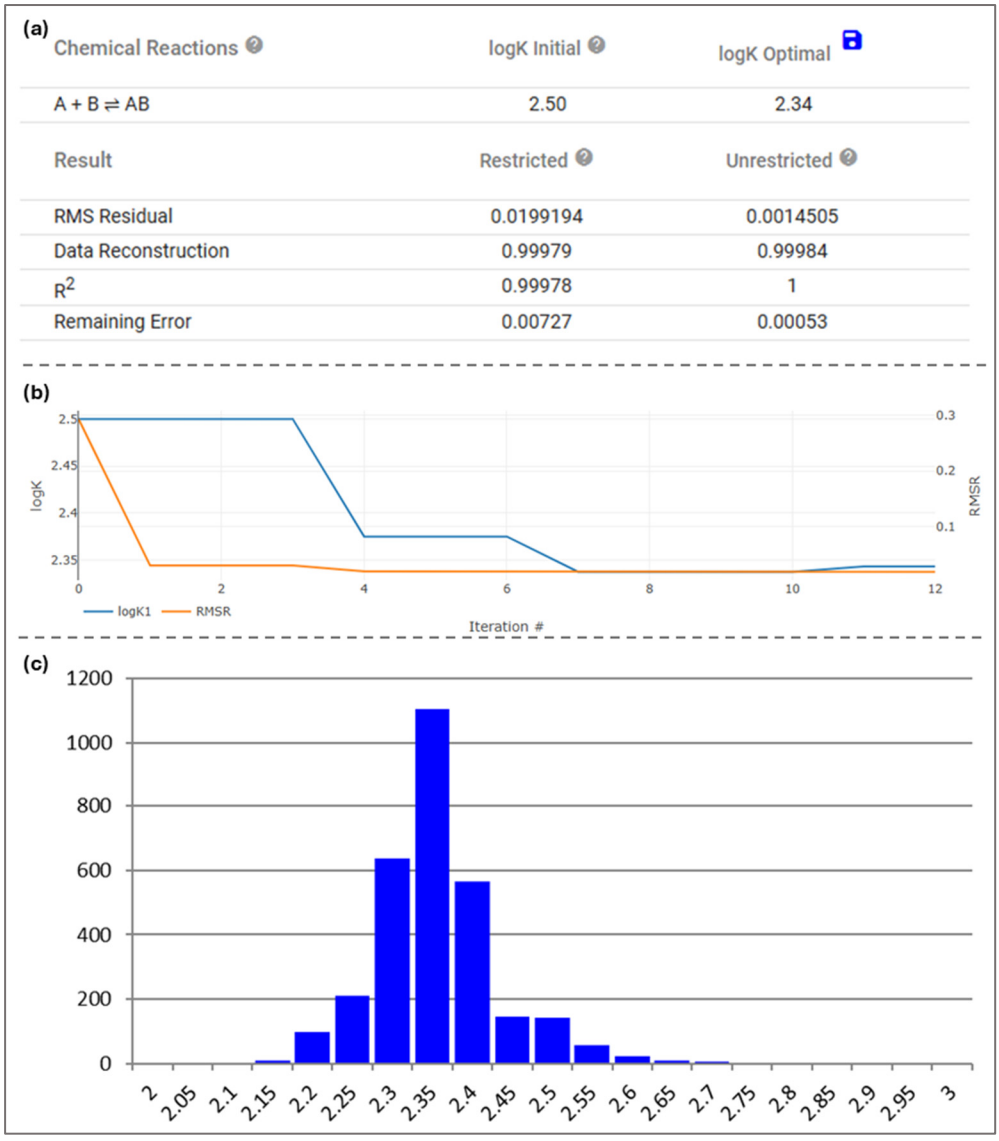

Figure S33. Representative (a) summary table, (b) fitted data, and (c) combined histograms (1000 bootstraps for each trial) for uncertainty analysis for H-IPr·PF_6 (1.3 mM) with Cl^- in dry acetone-d_6.

Table S12. Summary of ^{1}H NMR titration data for H-IPr·PF_6 (1.3 mM) and TBACl in dry acetone-d_6.

Trial	log $K_{1:1}$	95% confidence interval
1	2.31	[2.18, 2.49]
2	2.32	[2.19, 2.48]
3	2.34	[2.18, 2.53]
Average	2.32	[2.19, 2.51]

S1.3.3.3 Details and results of ^{1}H NMR titration for H-IPr·PF_6 (48.9 mM) and TBACl

Table S13. Representative titration data of H-IPr·PF_6 (48.9 mM) with Cl^-.

	V guest (µL)	equiv. guest	[host] (M)	[guest] (M)	δ1 (ppm)	δ2 (ppm)	δ3 (ppm)
1	0	0.00	0.0489	0.000	9.7916	8.4283	7.5578
2	2	0.08	0.0489	0.00382	9.9018	8.4260	7.5485
3	4	0.16	0.0489	0.00762	10.011	8.4259	7.5483
4	6	0.23	0.0489	0.01138	10.1079	8.4238	7.5422
5	8	0.31	0.0489	0.0151	10.1991	8.4232	7.5395
6	10	0.38	0.0489	0.0188	10.2808	8.4223	7.5354
7	15	0.57	0.0489	0.0279	10.4527	8.4216	7.5287
8	20	0.75	0.0489	0.0369	10.6023	8.4207	7.5220
9	25	0.93	0.0489	0.0457	10.7301	8.4201	7.5162
10	30	1.11	0.0489	0.0543	10.8433	8.4212	7.5123
11	35	1.28	0.0489	0.0628	10.9419	8.4216	7.5081
12	60	2.10	0.0489	0.103	11.1146	8.4226	7.5002
13	85	2.85	0.0489	0.139	11.2546	8.4235	7.4948
14	110	3.54	0.0489	0.173	11.3743	8.4287	7.4904
15	135	4.17	0.0489	0.204	11.4765	8.4319	7.4861
16	160	4.76	0.0489	0.233	11.5652	8.4352	7.4820

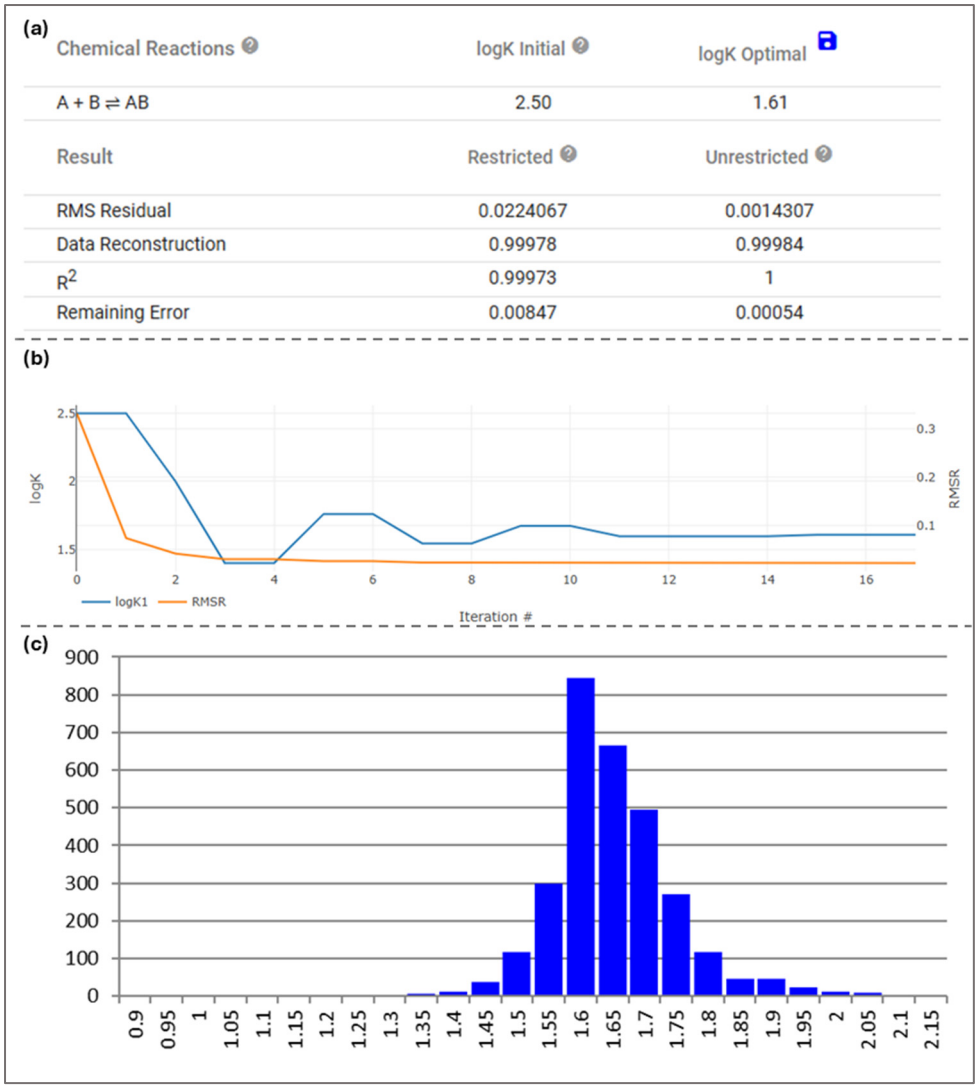

Figure S34. Representative (a) summary table, (b) fitted data, and (c) combined histograms (1000 bootstraps for each trial) for uncertainty analysis for H-IPr·PF_6 (48.9 mM) with Cl^- in dry acetone-d_6.

Table S14. Summary of ^{1}H NMR titration data for H-IPr·PF_6 (48.9 mM) and TBACl in dry acetone-d_6.

Trial	log $K_{1:1}$	95% confidence interval
1	1.59	[1.46, 1.89]
2	1.57	[1.47, 1.85]
3	1.61	[1.47, 1.85]
Average	1.59	[1.46, 1.87]

S1.3.3.4 Details and results of ^{1}H NMR titration for *p*-CF_3-tren-trisurea (14.1 mM) with $TBANO_3$

Table S15. Representative titration data of *p*-CF_3-tren-trisurea (14.1 mM) with NO_3^-.

	V guest (µL)	equiv. guest	[host] (M)	[guest] (M)	δ1 (ppm)	δ2 (ppm)	δ3 (ppm)
1	0	0.00	0.0141	0.000	8.5799	7.4782	6.1775
2	2	0.05	0.0141	0.000772	8.5863	7.4817	6.1857
3	4	0.11	0.0141	0.00154	8.5918	7.4845	6.1951
4	6	0.16	0.0141	0.00230	8.5967	7.4868	6.2033
5	8	0.22	0.0141	0.00305	8.6021	7.4897	6.2118
6	10	0.27	0.0141	0.00380	8.6073	7.4922	6.2200
7	15	0.40	0.0141	0.00564	8.6197	7.4980	6.2392
8	20	0.53	0.0141	0.00745	8.6301	7.5024	6.2556
9	25	0.66	0.0141	0.00923	8.6402	7.5071	6.2712
10	30	0.78	0.0141	0.0110	8.6499	7.5118	6.2859
11	35	0.90	0.0141	0.0127	8.6585	7.5154	6.2988
12	45	1.14	0.0141	0.0160	8.6734	7.5218	6.3214
13	55	1.36	0.0141	0.0192	8.6865	7.5277	6.3409
14	65	1.58	0.0141	0.0223	8.6984	7.5323	6.3571
15	75	1.80	0.0141	0.0253	8.7083	7.5362	6.3714
16	85	2.00	0.0141	0.0281	8.7171	7.5398	6.3836
17	110	2.48	0.0141	0.0349	8.7349	7.5460	6.4073

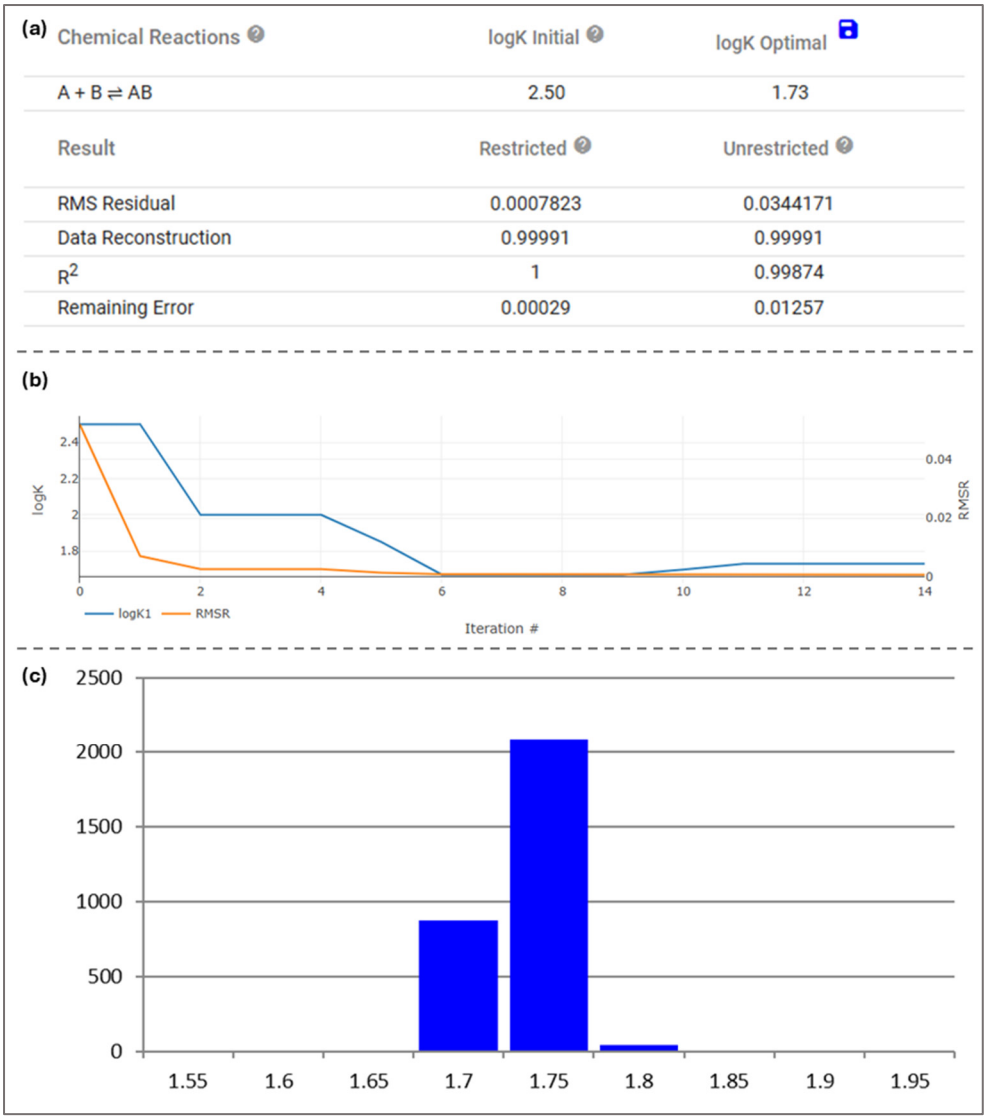

Figure S35. Representative (a) summary table, (b) fitted data, and (c) combined histograms (1000 bootstraps for each trial) for uncertainty analysis for *p*-CF_3-tren (*tris*)urea (14.1 mM) and $TBANO_3$ in dry 20% DMSO-d_6 in MeCN-d_3 solution.

Table S16. Summary of ^{1}H NMR titration data for *p*-CF_3-tren (*tris*)urea (14.1 mM) and $TBANO_3$ in dry 20% DMSO-d_6 in MeCN-d_3 solution.

Trial	log $K_{1:1}$	95% confidence interval
1	1.72	[1.70, 1.73]
2	1.71	[1.69, 1.73]
3	1.73	[1.69, 1.76]
Average	1.72	[1.69, 1.74]

S1.3.3.5 Details and results of ^{1}H NMR titration for *p*-CF_3-tren-trisurea (14.1 mM) with $TBAHSO_4$

Table S17. Representative titration data of *p*-CF_3-tren-trisurea (14.1 mM) with HSO_4^-.

	V guest (µL)	equiv. guest	[host] (M)	[guest] (M)	δ1 (ppm)	δ2 (ppm)	δ3 (ppm)
1	0	0.00	0.0141	0.000	8.5929	7.4835	6.1777
2	2	0.05	0.0141	0.000763	8.6917	7.4948	6.3198
3	4	0.11	0.0141	0.00152	8.7959	7.5076	6.4553
4	6	0.16	0.0141	0.00227	8.9082	7.5232	6.5798
5	8	0.21	0.0141	0.00301	9.0026	7.5249	6.7268
6	10	0.27	0.0141	0.00375	9.1036	7.5355	6.8592
7	15	0.39	0.0141	0.00558	9.3044	7.5514	7.1068
8	20	0.52	0.0141	0.00736	9.3980	7.5522	7.2503
9	25	0.65	0.0141	0.00912	9.4352	7.5518	7.3116
10	30	0.77	0.0141	0.0108	9.4569	7.5530	7.3460
11	35	0.89	0.0141	0.0125	9.4737	7.556	7.3714
12	40	1.00	0.0141	0.0142	9.4851	7.5568	7.3881
13	45	1.12	0.0141	0.0158	9.4956	7.5584	7.4032
14	50	1.23	0.0141	0.0174	9.5041	7.5595	7.4151
15	55	1.34	0.0141	0.0190	9.5110	7.5595	7.4247
16	60	1.45	0.0141	0.0205	9.5190	7.5621	7.4351
17	70	1.66	0.0141	0.0235	9.5270	7.5623	7.4455
18	80	1.87	0.0141	0.0264	9.5382	7.5643	7.4597

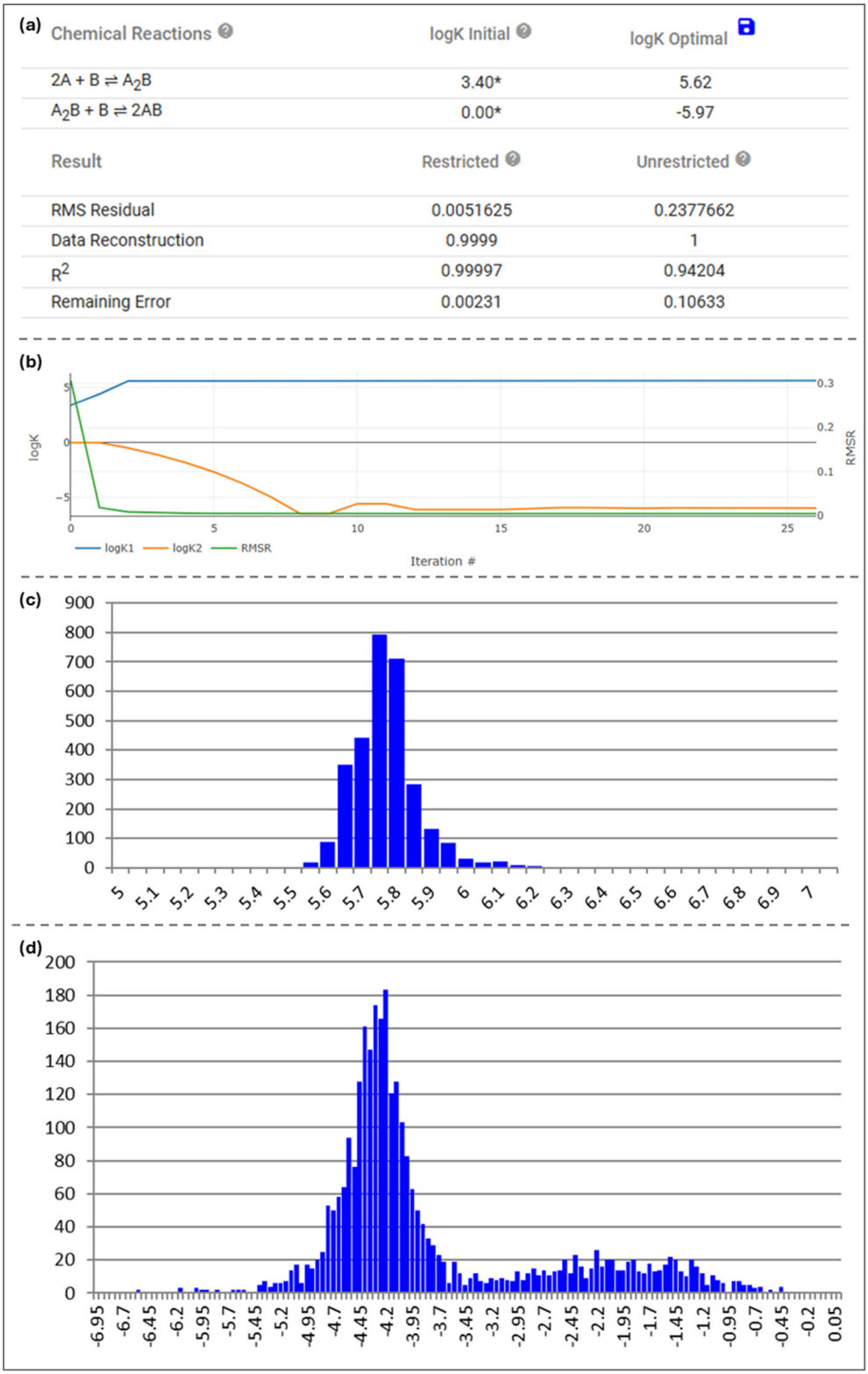

Figure S36. Representative (a) summary table, (b) fitted data, and (c,d) combined histograms (1000 bootstraps for each trial) for uncertainty analysis for $K_{2:1}$ and $K_{1:1}$ (c and d) for *p*-CF_3-tren-*tris*urea (14.1 mM) and $TBAHSO_4$ in dry 20% DMSO-d_6 in MeCN-d_3 solution.

Table S18. Summary of ^{1}H NMR titration data for *p*-CF_3-tren-*tris*urea (14.1 mM) and $TBAHSO_4$ in dry 20% DMSO-d_6 in MeCN-d_3 solution.

Trial	log $K_{2:1}$	95% confidence interval	log $K_{1:1}$	95% confidence interval
1	5.62	[5.59, 6.02]	−5.97	[−6.97, −1.03]
2	5.71	[5.59, 5.96]	−5.55	[−6.18, −1.22]
3	5.74	[5.59, 5.96]	−4.32	[−5.12, −1.23]
Average	5.69	[5.59, 5.98]	−5.28	[−5.20, −1.15]

S1.3.3.6 Details and results of ^{1}H NMR titration for *p*-CF_3-tren-trisurea (14.1 mM) with TBAOCN

Table S19. Representative titration data of *p*-CF_3-tren-trisurea (14.1 mM) with OCN^-.

	V guest (µL)	equiv. guest	[host] (M)	[guest] (M)	δ1 (ppm)	δ2 (ppm)	δ3 (ppm)
1	0	0	0.0141	0.000	8.5830	7.4819	6.1804
2	2	0.08	0.0141	0.00111	8.6318	7.4893	6.2189
3	4	0.16	0.0141	0.00221	8.6793	7.4973	6.2468
4	6	0.23	0.0141	0.00330	8.7272	7.5046	6.2638
5	8	0.31	0.0141	0.00438	8.7750	7.5124	6.2906
6	10	0.39	0.0141	0.00546	8.8212	7.5200	6.3169
7	15	0.57	0.0141	0.00812	8.9343	7.5378	6.3814
8	20	0.76	0.0141	0.0107	9.0398	7.5544	6.4404
9	25	0.94	0.0141	0.0133	9.1284	7.5676	6.4885
10	30	1.12	0.0141	0.0158	9.1934	7.5759	6.5213
11	35	1.29	0.0141	0.0182	9.2401	7.5800	6.5419
12	45	1.63	0.0141	0.0230	9.3092	7.5844	6.5695
13	55	1.95	0.0141	0.0276	9.3681	7.5868	6.5907
14	65	2.27	0.0141	0.0320	9.3926	7.588	6.5998
15	75	2.57	0.0141	0.0363	9.4385	7.5898	6.6212
16	85	2.86	0.0141	0.0404	9.4842	7.5911	6.6310

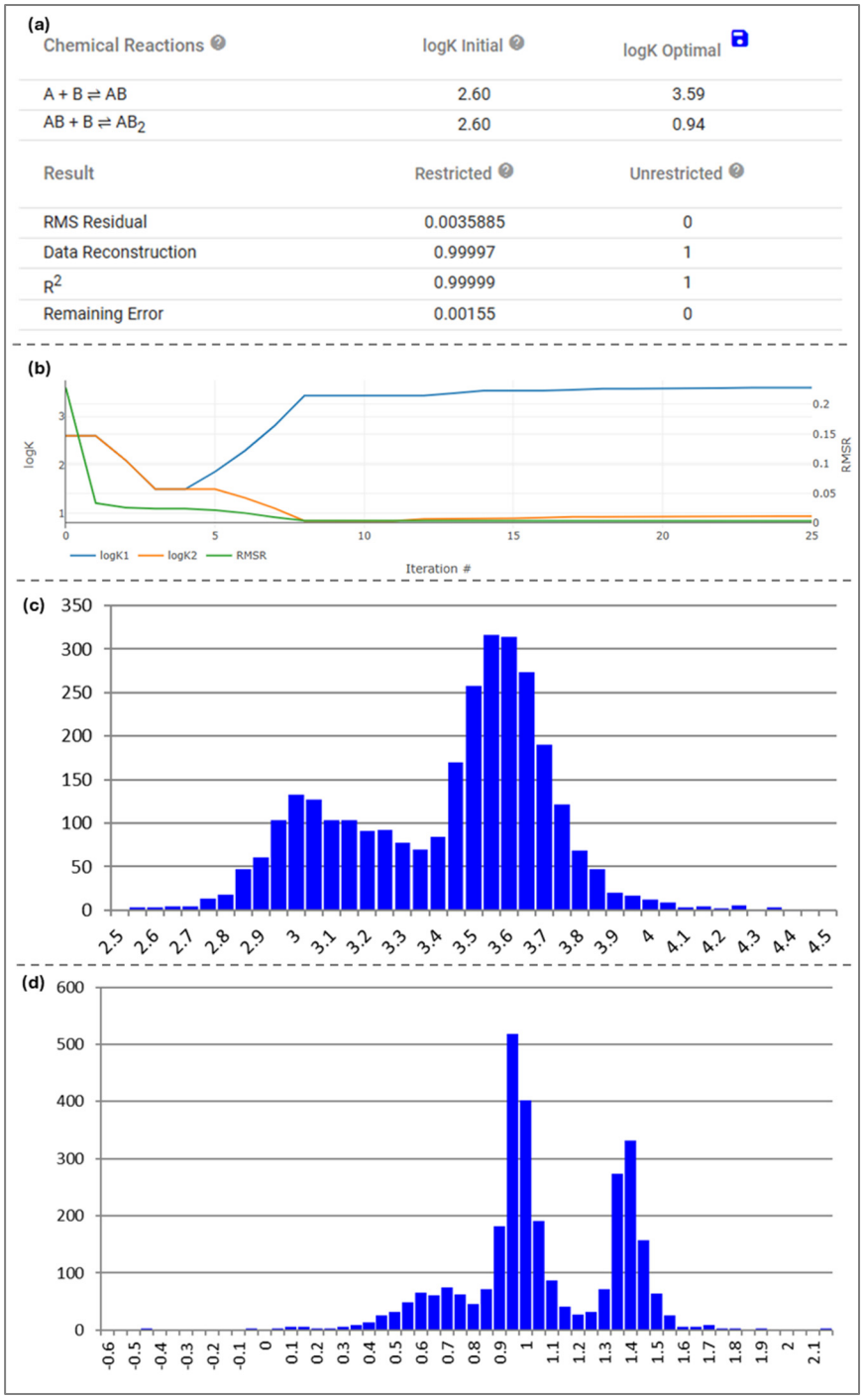

Figure S37. Representative (a) summary table, (b) fitted data, and (c,d) combined histograms (1000 bootstraps for each trial) for uncertainty analysis for $K_{1:1}$ and $K_{1:2}$ (c and d) for *p*-CF_3-tren (*tris*)urea (14.1 mM) and TBAOCN in dry 20% DMSO-d_6 in MeCN-d_3 solution.

Table S20. Summary of ^{1}H NMR titration data for *p*-CF_3-tren (*tris*)urea (14.1 mM) and TBAOCN in dry 20% DMSO-d_6 in MeCN-d_3 solution.

Trial	log $K_{1:1}$	95% confidence interval	log $K_{1:2}$	95% confidence interval
1	2.98	[2.74, 3.57]	1.35	[0.91, 1.54]
2	3.45	[3.24, 3.96]	0.64	[0.36, 1.14]
3	3.59	[3.28, 3.96]	0.94	[0.35, 1.24]
Average	3.34	[2.84, 3.95]	0.98	[0.40, 1.48]

S1.3.4 UV-vis titrations

UV-vis titration data were collected at 25 °C on a Cary 60 instrument. Before each titration experiment, a background of the acetonitrile (ACS grade) in a quartz cuvette (1.0 cm) sealed with a septa cap was collected. A stock solution of the host compound NBS (2.20 mM) in MeCN was prepared. To maintain a constant host concentration during the course of titration, guest (TBABr) was dissolved in 1.0 mL of the host solution.[5] The guest solution (TBABr) was added to the host solution using a microsyringe and allowed to equilibrate for 1 minute before data collection. The titration data were subjected to using parametric equilibrium-restricted global analysis (PERGA) using the SIVVU program.[6] Different fitting models were tested to confirm the best fit from each set of data. Titrations were performed in triplicate, where the final values reported in each table are the average of K_a and the histogram of combined 95% confidence intervals for the three titrations.[7]

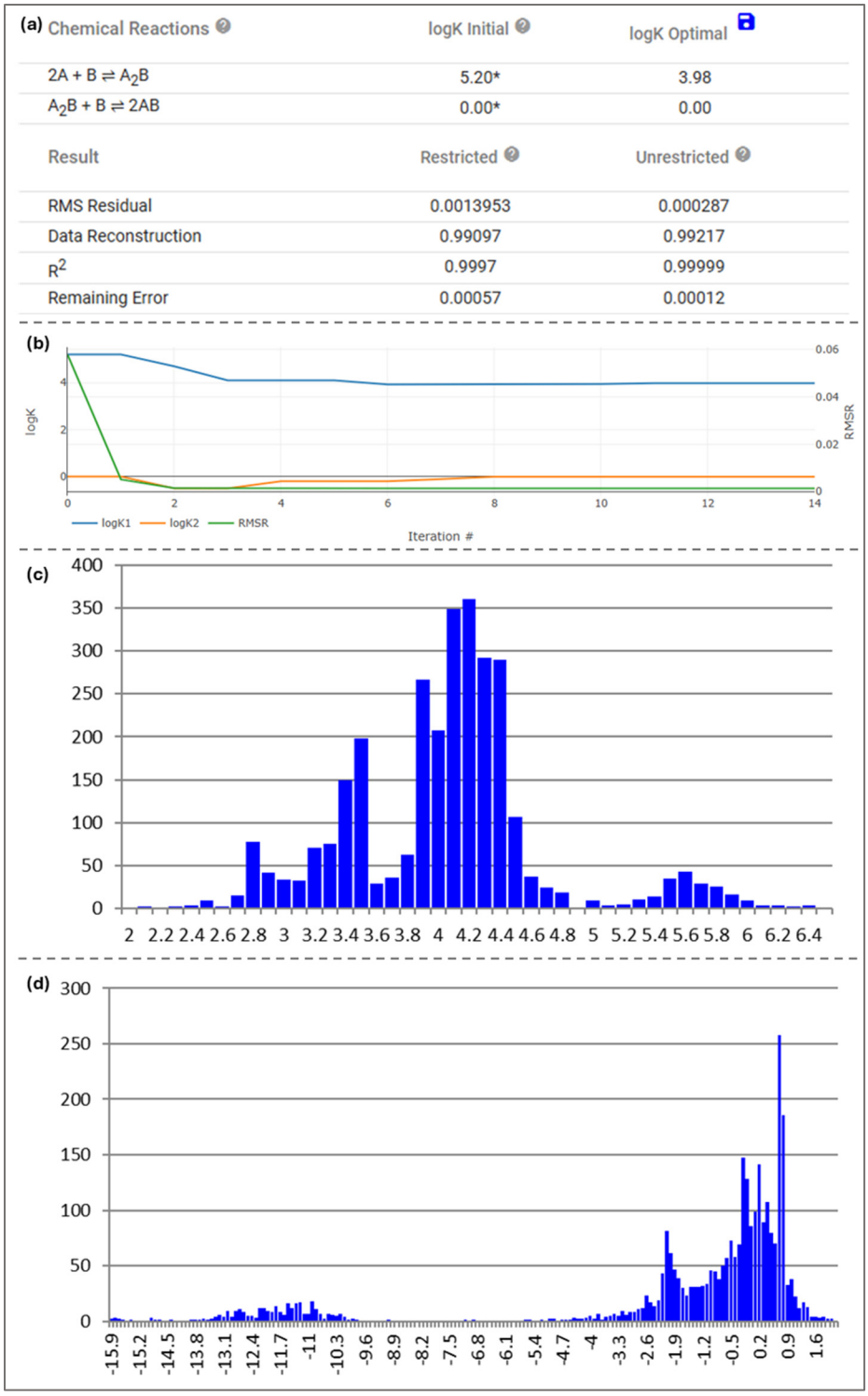

Figure S38. Representative (a) summary table, (b) fitted data, and (c,d) combined histograms (1000 bootstraps for each trial) for uncertainty analysis for $K_{2:1}$ and $K_{1:1}$ (c and d) for NBS (2.20 mM) and TBABr in MeCN solution.

Table **S21**. Summary of UV-vis titration data for NBS (2.20 mM) and TBABr in MeCN solution.

Trial	log $K_{2:1}$	95% confidence interval	log $K_{1:1}$	95% confidence interval
1	3.88	[2.78, 5.33]	0.66	[−1.31, 1.00]
2	4.26	[3.92, 5.75]	−3.34	[−16.22, −0.25]
3	3.98	[2.65, 4.63]	0.00	[−10.96, 1.30]
Average	4.04	[2.79, 5.68]	−0.89	[−13.20, 1.10]

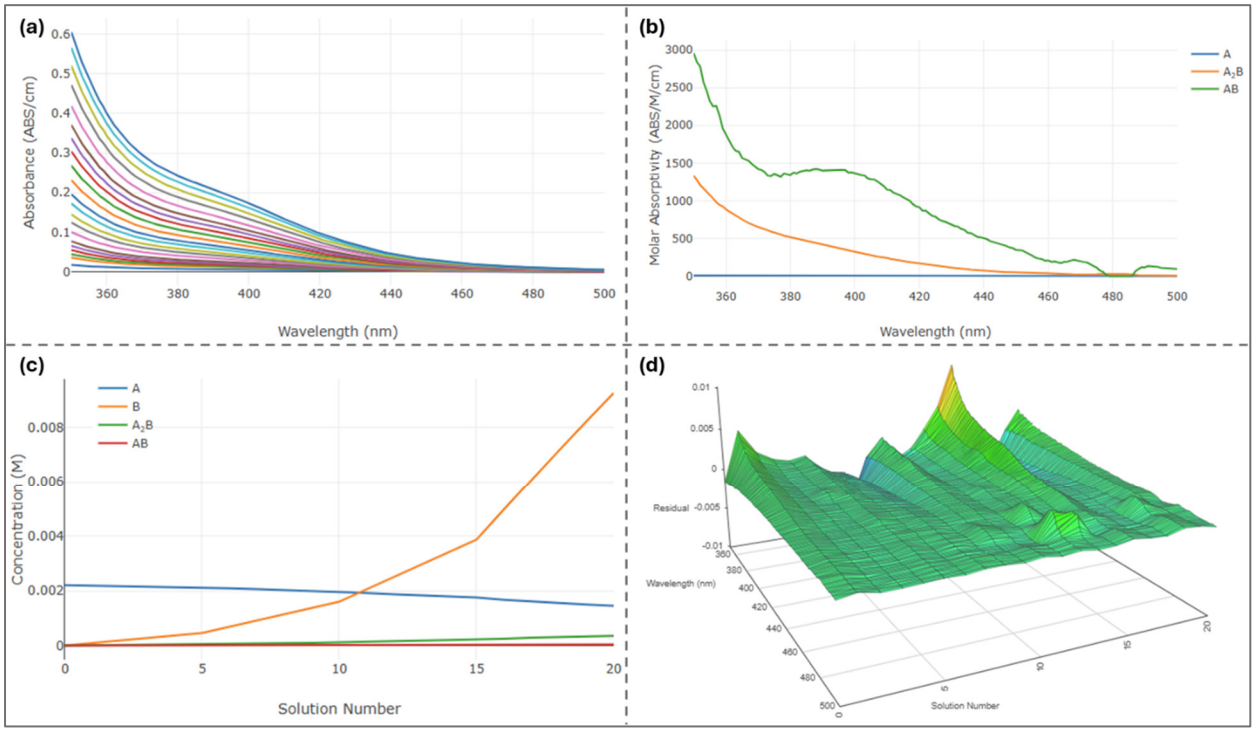

Figure S39. (a) UV-vis titration spectra of NBS (2.20 mM) and TBABr in MeCN solution mixture at 298 K. (b) Molar absorptivity plots of the host (blue), 2:1 host-guest complex (yellow), and 1:1 host-guest complex (green). (c) Concentration data of different host (A, blue), guest (B, yellow), 2:1 host-guest complex (A_2B, green), and 1:1 host-guest complex (AB, red). (d) Residuals obtained from data fitting.

S1.3.5 ATR-FTIR

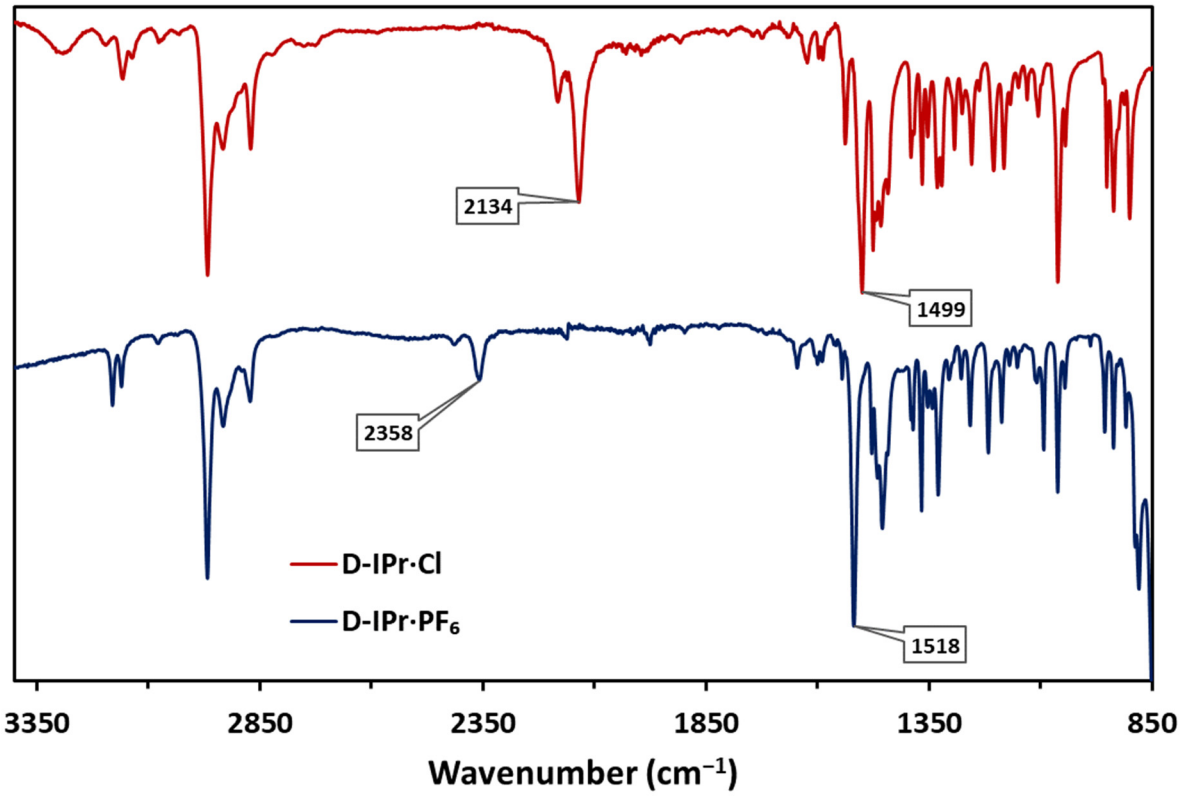

Figure S40. *Di*-ATR-FTIR of solid compounds D-IPr·Cl (top, red trace), and D-IPr·PF_6 (bottom, blue trace).

S1.4 References

(1) Jafarpour, L.; Stevens, E. D.; Nolan, S. P. A Sterically Demanding Nucleophilic Carbene: 1,3-Bis(2,6-Diisopropylphenyl)Imidazol-2-Ylidene). Thermochemistry and Catalytic Application in Olefin Metathesis. *J. Organomet. Chem.* **2000**, *606* (1), 49–54. https://doi.org/10.1016/S0022-328X(00)00260-6.

(2) Wei, S.; Wei, X.-G.; Su, X.; You, J.; Ren, Y. Insight into the Role of the Counteranion of an Imidazolium Salt in Organocatalysis: A Combined Experimental and Computational Study. *Chem. – Eur. J.* **2011**, *17* (21), 5965–5971. https://doi.org/10.1002/chem.201002839.

(3) Busschaert, N.; Wenzel, M.; Light, M. E.; Iglesias-Hernández, P.; Pérez-Tomás, R.; Gale, P. A. Structure–Activity Relationships in Tripodal Transmembrane Anion Transporters: The Effect of Fluorination. *J. Am. Chem. Soc.* **2011**, *133* (35), 14136–14148. https://doi.org/10.1021/ja205884y.

(4) Cicač-Hudi, M.; Bender, J.; Schlindwein, S. H.; Bispinghoff, M.; Nieger, M.; Grützmacher, H.; Gudat, D. Direct Access to Inversely Polarized Phosphaalkenes from Elemental Phosphorus or Polyphosphides. *Eur. J. Inorg. Chem.* **2016**, *2016* (5), 649–658. https://doi.org/10.1002/ejic.201501017.

(5) Connors, K. A. Binding Constants: The Measurement of Molecular Complex Stability; Wiley, 1987.

(6) Vander Griend, D.A.; DeVries, M. J.; Greeley, M.; Kim, Y.; Wang, N.; Buist, D; Ulry, C. SIVVU, http://sivvu.org, 2021

(7) Lawler, F. C.; Storteboom, R. S.; Rosales-Lopez, P. D.; Hoogstra, M. N.; Selvaggio, K. J.; Chen, T.; Zogg, K. A.; Heule, D. L.; Pehrson, N. J.; Baker, A. E.; Vander Griend, D. A. On the Replicability of the Thermodynamic Modeling of Spectroscopic Titration Data in the Nickel(II) En System. *Journal of Chemometrics* **2024**, *38* (12), e3619. https://doi.org/10.1002/cem.3619.